



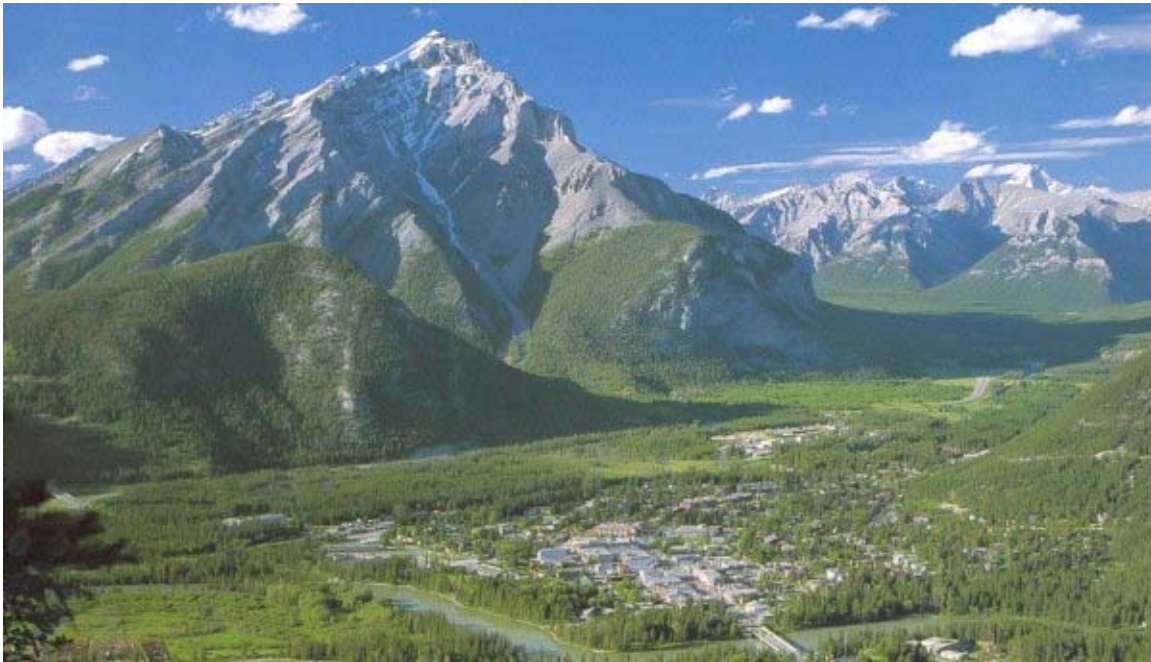
Banff International Research Station
for Mathematical Innovation and Discovery

***Physics-Based Mathematical Models of Low-Dimensional
Semiconductor Nanostructures: Analysis and Computation***

November 18-23, 2007

Organizers: Lok Lew Yan Voon (Wright State University), Roderick Melnik (Wilfrid Laurier University), Morten Willatzen (University of Southern Denmark)

PROGRAM AND ABSTRACTS



OBJECTIVES

This workshop is devoted to physics-based mathematical models for the description of low-dimensional semiconductor nanostructures (LDSNs) that are becoming increasingly important in technological innovations. It is an area where fundamental questions of experimental techniques, physical insight, applied mathematics and design of computational methodologies are meeting together in a quest for an adequate description of nanostructures which have very promising properties for applications.

The workshop is aimed at bringing together researchers working on different aspects of the analysis, experiment and modeling of LDSNs. The problem of predicting accurately optoelectromechanical properties of LDSNs requires a concerted effort of teams of researchers with close interactions between physicists, applied mathematicians and computational scientists. The main objective of the workshop is to bring together the leading experts in the field from each of these communities in order to

- (a) summarize the most recent experimental achievements in the LDSN area with associated physical effects and phenomena that require better understanding,
- (b) summarize the state-of-the-art models and computational techniques for modeling LDSNs that can assist further progress in key areas of LDSN applications,
- (c) identify critical problems of major importance and prioritize them,
- (d) analyze the feasibility of existing mathematical and computational methodologies for the solution of some such problems, and
- (e) use the workshop working sessions to explore promising approaches in addressing identified challenges.

At the beginning of the workshop, state-of-the-art overviews of the subject from perspectives of physics, applied mathematics and computational science communities will be given by key experts in their respective fields. Such overviews should help better refine the areas where joint efforts are needed in addressing key challenges in LDSNs, both theoretical and experimental, and where such efforts would be the most productive. During the week of working sessions in the stimulating environment of the Banff International Research Station, the participants of the workshop will be engaged in collaborative interdisciplinary projects, focusing on the identified key research priorities in the development of physics-based models for LDSNs, experimental areas, and LDSN applications. All participants will have time to present their current research on LDSNs and a specific time will be allocated for on-site demonstrations of software and explanations of experimental tools applied in the LDSN analysis. The BIRS has a report series for surveys of the status of the subjects of the workshops and, with help of the workshop participants, we will ensure a wide dissemination of the workshop outcomes. In addition, some of the talks will be video-taped by BIRS for dissemination through video-streaming on the Internet, and for archival purposes. Finally, in order to stimulate initial discussions, prior to the workshop a web-based LDSN Comptes Rendus will be set up, an electronic resource, in which the participants of the workshop will be encouraged to deposit their preprints, reprints and manuscripts on the topics of the workshop.

FACILITIES

The *Banff International Research Station* is physically located on the campus of the Banff Centre. BIRS occupies all of *Corbett Hall* and the lower half of the adjoining *Max Bell Building*. Both parts of the facility are wheel-chair accessible.



Corbett Hall



Max Bell complex

Accommodation: Participants of BIRS programmes are housed in Corbett Hall, which has 50 rooms. Each room has a queen-sized bed, a Sun Ray terminal connected to the BIRS computer system as well as the Internet, an ethernet port for laptops, and a desk. The majority of rooms share a bathroom with one other room. We make an effort to keep each pair all male/all female.

Corbett Hall 5210 - Common Lounge: Where coffee breaks are taken. Espresso and other snacks are available, with contributions made on an honours system. The lounge is accessible 24 hours/day so participants can relax in it at any time - there is a sofa, fireplace, some board games and a television (in addition to some tables.)

Corbett Hall 5310 - Reading Room: A good place to sit quietly and study. There are two PCs connected to the network as well as a scanner, a network printer, one Sun Ray terminal connected to the BIRS computer system, several ethernet ports, wireless networking and a white board.

Corbett Hall 5110 - Main Office:

- copier
- fax machine
- office supplies

The Main Office is the location of the offices of the Station Manager, Station Facilitator and Systems Analyst.

The Max Bell complex has 5 rooms reserved exclusively for the use of BIRS programmes.

Max Bell Room 159 - Main Lecture Room: Most workshop lectures are held here. The room has:

- a ceiling-mounted LCD Projector with remote control
- two overhead projectors
- two projection screens
- a digital document camera
- three chalkboards
- wireless Internet access

Capacity: 42

Max Bell Room 158 - Small Lecture Room:

- one overhead projector
- a large projection screen

Capacity: 18

Max Bell Room 157 - Terminal Room:

- a projection screen
- 1 whiteboard
- 6 Sun Ray Terminals with Internet Access

Capacity: 8

Max Bell Room 156 - Small Lecture Room:

- a large projection screen
- 1 chalkboard

Capacity: 22

Max Bell Room 155 - Small Discussion Room:

- a projection screen
- 1 whiteboard
- an upright piano

Capacity: 6

Poster Wall: This is a 5 meter (length wise) magnetic wall in the hallway outside the lecture rooms on which posters may be displayed for the duration of a workshop.

Computer Networks: The BIRS computing environment consists of two networks, one for thin-client Sun Ray terminals, and one for direct connectivity to the Internet via the Banff Centre's network.

The Sun Rays have 15" LCD panels with a keyboard, mouse and network connection. They have no moving parts, so they are completely silent. They connect to a central Sun server that runs Solaris 10 and the GNOME 2.6 desktop environment. The full suite of standard UNIX software is installed, as well as the most popular tools for mathematics

publishing. The high-speed, permanent Internet connection and a robust selection of Internet software is always available via these terminals.

The guest network for laptops is a fast ethernet network, with ports available in all bedrooms, in most meeting areas, and in the main lecture room. Configuration for network access is done automatically via DHCP. The guest network is also accessible via wireless networking (802.11b/g) in all areas of BIRS.

Library: BIRS has a very small, but growing, library. It has online access to MathSciNet. Participants who have online services at their home institutions are encouraged to establish proxy accounts which will allow them journal access from BIRS.

The Banff Centre has a very nice arts/music library which has a good collection of sheet music as well as recorded music and video material. BIRS participants are welcome to use this library.

The Banff Centre: The Banff Centre is a centre for fine arts programmes, leadership development, mountain culture, and, since 2003, BIRS. It is situated in the town of Banff part way up Tunnel Mountain on a peaceful and secluded site.

It has an athletic complex with swimming pool, running track, workout room, climbing wall etc. All of which are available to BIRS participants. For more on the Banff Centre and its current artistic programme, please refer to the Banff Centre webpage <http://www.banffcentre.ca>.

During your stay at BIRS, you can be contacted by telephone through The Banff Centre switchboard, which is open 24 hours, at +1-403-762-6100.

PARTICIPANT ACCOMMODATION

Participants of BIRS programmes are housed in Corbett Hall at the Banff Centre. 5-day workshop participants are expected to arrive on Sunday afternoon or evening (check-in is after 4 p.m.) and to depart Friday midday (check-out is at noon). Accommodation and meals are provided for the organizers and participants for this period.

Check-in desk at the Banff Centre is located in the Professional Development Centre (PDC). The desk is open 24 hours so participants can check in anytime. Here you will be given the key to your room in Corbett Hall as well as any information useful for BIRS participants. During your stay at BIRS, you can be contacted by telephone through The Banff Centre switchboard, which is open 24 hours, at +1-403-762-6100.

For detailed information on the set up at BIRS please go to the Facilities section on the home page. Participants of BIRS programmes are housed in Corbett Hall, which has 50 rooms. Each room has one queen-sized bed, a telephone, a SunRay terminal connected to the BIRS computer system and the Internet, an ethernet port with a cable for laptops, and a desk. There are also wireless access points in some common areas. Most bedrooms share a bathroom with one other bedroom. Corbett Hall has 4 floors and is not equipped with an elevator. If you feel that this could be a physical challenge to you, please advise us and we will be happy to accommodate you on a lower floor.

PARTICIPANTS

| | | |
|-------------------------|--|--------------------------------------|
| Arakawa, Yasuhiko | University of Tokyo | arakawa@iis.u-tokyo.ac.jp |
| Austing, David | National Research Council of Canada | guy.austing@nrc-cnrc.gc.ca |
| Barettin, Daniele | University of Southern Denmark | Daniele@mci.sdu.dk |
| Birner, Stefan | Walter Schottky Institute, Technical University of Munich | stefan.birner@wsi.tum.de |
| Brown, Gail | Air Force Research Lab, Wright- Patterson AFB | Gail.Brown@WPAFB.AF.MIL |
| Caflich, Russel | University of California at Los Angeles | caflisch@math.ucla.edu |
| Chrzan, Daryl | University of California at Berkeley | dcchrzan@berkeley.edu |
| Chuang, Shun Lien | University of Illinois at Urbana- Champaign | s-chuang@uiuc.edu |
| Clarke, Edmund | Imperial College London | edmund.clarke@imperial.ac.uk |
| Guo, Hong | McGill University | guo@physics.mcgill.ca |
| Houmark, Jakob | Technical University of Denmark | Jakob.Houmark@mic.dtu.dk |
| Huang, Hanchen | Rensselaer Polytechnic Institute | huangh@rpi.edu |
| Jauho, Antti-Pekka | Technical University of Denmark | antti@mic.dtu.dk |
| Johnson, Harley | University of Illinois at Urbana- Champaign | htj@uiuc.edu |
| Klimeck, Gerhard | Purdue University | gekco@exchange.purdue.edu |
| Korkusinski, Marek | National Research Council of Canada | Marek.Korkusinski@nrc- cnrc.gc.ca |
| Kyriakidis, Jordan | Dalhousie University | jordan.kyriakidis@dal.ca |
| Lassen, Benny | University of Southern Denmark | benny@mci.sdu.dk |
| Lew, Adrian | Stanford University | lewa@stanford.edu |
| Lew Yan Voon, Lok | Wright State University | lok.lewyanvoon@wright.edu |
| Li, Shaofan | University of California, Berkeley | li@ce.berkeley.edu |
| Melnik, Roderick | Wilfrid Laurier University | rmelnik@wlu.ca |
| Neophytou, Neophytos | Purdue University | neophyto@ecn.purdue.edu |
| Niu, Xiaobin | University of California at Los Angeles | xbniu@ucla.edu |
| O'Reilly, Eoin | Tyndall National Institute | eoin.oreilly@tyndall.ie |
| Park, Harold | University of Colorado | harold.park@vanderbilt.edu |

| | | |
|------------------------------|--|----------------------------------|
| Pedesseau, Laurent | L'INSA de Rennes - France | laurent.pedesseau@insa-rennes.fr |
| Roy Mahapatra, Debiprosad | Indian Institute of Science | droymahapatra@aero.iisc.ernet.in |
| Schirmer, Sonia | University of Cambridge | sgs29@cam.ac.uk |
| Uskov, Alexander | Lebedev Physical Institute | alexusk@lebedev.ru |
| Vasileska, Dragica | Arizona State University | Vasileska@asu.edu |
| Voss, Frands | University of Southern Denmark | voss@mci.sdu.dk |
| Wang, Lin-Wang | Lawrence Berkeley National Laboratory | lwwang@lbl.gov |
| Willatzen, Morten | University of Southern Denmark | willatzen@mci.sdu.dk |
| Zhang, Yong | NREL of the U.S. Department of Energy | yong_zhang@nrel.gov |
| Zhou, Min | Georgia Tech | min.zhou@me.gatech.edu |

TALKS AND DISCUSSIONS

Plenary talks will be up to a max of 40 mins with 5 mins questions, regular talks will be around 15 mins with 5 mins questions. There will be additional time for discussions in the afternoon. Topics for the study groups will be announced and sign-up sheets posted onsite.

You can submit further your comments on the topics of the workshop to your folder at the LDSN eprint site (and, of course, open problems are still very welcome and needed!). Also, we would like to encourage the submission of your presentations to the same site. Finally, we would like to encourage you to submit your preprints and reprints relevant to this LDSN workshop (not necessarily on the topic of your main presentation at Banff, but of relevance to the topics of this workshop). It will help to share the information between the participants of this workshop as well as networking. We remind you that the site for all these submissions is at <http://www.m2netlab.wlu.ca/ldsn-banff/eprints.php> (please take your username and password with you as you can continue downloading the files during the workshop - wireless access will be available throughout the Banff International Research Station).

PROCEEDINGS

All participants are encouraged to submit their work for publication in a proceedings. Original (research and review) articles will be published online in the Journal of Physics: Conference Series with open access. Manuscripts should be emailed to the organizers and will be peer-reviewed. Deadline for submission will be December 15, 2007. There is no page limit.

Guidelines for manuscript preparation:

- (1) We only need a PDF of each accepted paper, prepared according to the guidelines outlined below.
- (2) There are templates in Word and LaTeX plus quite comprehensive guidelines on PDF preparation from the publisher.

(a) LaTeX templates

<http://ej.iop.org/pdf/jpconf/jpcslatexguidelines.zip>

(b) Word templates

<http://ej.iop.org/pdf/jpconf/jpcswordguidelines.zip>

(c) PDF preparation guidelines

<http://www.iop.org/ej/journal/-page=extra.4/1742-6596>

(d) Key items to consider if authors do not want to use the templates

We prefer authors to use their templates but do not insist on it. You are free to use any software/templates of their choice provided these key guidelines are adhered to:

<http://www.iop.org/EJ/journal/-page=extra.5/1742-6596>

SCHEDULE

MEALS

*Breakfast (Buffet): 7:00 – 9:00 am, Sally Borden Building, Monday – Friday

*Lunch (Buffet): 11:30 am – 1:30 pm, Sally Borden Building, Monday – Friday

*Dinner (Buffet): 5:30 – 7:30 pm, Sally Borden Building, Sunday – Thursday

Coffee Breaks: As per daily schedule, 2nd floor lounge, Corbett Hall

***Please remember to scan your meal card at the host/hostess station in the dining room for each meal.**

MEETING ROOMS

All lectures will be held in Max Bell 159 (Max Bell Building accessible by bridge on 2nd floor of Corbett Hall). LCD projector, overhead projectors and blackboards are available for presentations. *Please note that the meeting space designated for BIRS is the lower level of Max Bell, Rooms 155-159. Please respect that all other space has been contracted to other Banff Centre guests, including any Food and Beverage in those areas.*

Sunday

16:00 Check-in begins (Front Desk – Professional Development Centre - open 24 hours)
17:30-19:30 Buffet Dinner, Sally Borden Building
20:00 Informal gathering in 2nd floor lounge, Corbett Hall.
Beverages and small assortment of snacks available on a cash honour-system.

Monday

7:00-8:45 Breakfast
8:45-9:00 Introduction and Welcome to BIRS by BIRS Station Manager, Max Bell 159
9:00-9:45 Plenary I (Caflisch)
9:45-10:45 Talk 1 (Huang, Lew)
10:45-11:00 Coffee break
11:00-12:00 Talk 2 (Johnson, Park, Zhou)
12:00-13:00 Lunch
13:00-14:00 Guided Tour of The Banff Centre; meet in the 2nd floor lounge, Corbett Hall
14:00-14:30 Group Photo; meet on the front steps of Corbett Hall
14:30-15:45 Study group
15:45-16:00 Coffee break
16:00-17:30 Discussion
18:00-19:30 Dinner (dining room opens at 17:30 daily)

Tuesday

7:00-9:00 Breakfast
9:00-9:45 Plenary II (Brown)
9:45-10:45 Talk 3 (Arakawa, Chuang, Clarke)

10:45-11:00 Coffee break
11:00-12:00 Talk 4 (Chrzan, Li, Zhang)
12:00-13:00 Lunch
13:00-13:45 Plenary III (Klimeck)
13:45-14:45 Talk 5 (Birner, Korkusinski, Wang)
14:45-15:45 Study group
15:45-16:00 Coffee break
16:00-17:30 Discussion
18:00-19:30 Dinner
19:30 Poster (Barettin, Houmark, Neophytou, Niu)

Wednesday

7:00-9:00 Breakfast
9:00-9:45 Plenary IV (Jauho)
9:45-10:45 Talk 6 (Austing, Guo, Vasileska)
10:45-11:00 Coffee break
11:00-12:00 Talk 7 (Kyriakidis, Schirmer, Uskov)
12:00-13:00 Lunch
13:00-14:00 Talk 8 (Lassen, Pedesseau, Roy)
14:00-15:30 Study group
15:30-16:00 Coffee break
16:00-17:30 Discussion
18:00-19:30 Dinner

Thursday

7:00-9:00 Breakfast
9:00-10:00 Talk 9 (nanoHUB.org presentation and demo - Klimeck)
10:00-10:15 Coffee break
10:15-12:00 Talk 10 (nextnano3 demo - Birner)
12:00-13:00 Lunch
13:00-18:00 Free
18:00-19:30 Dinner

Friday

7:00-9:00 Breakfast
9:00-10:00 Outcomes
10:00-10:15 Coffee break
10:15-11:15 Wrap up
11:30 Lunch

| | Sunday | Monday | Tuesday | Wednesday | Thursday | Friday |
|-------------|---------------|--------------------------------------|--------------------------------|-----------------------------------|-----------------------|---------------|
| 7:00-9:00 | | Breakfast Introduction (MB159) | Breakfast | Breakfast | Breakfast | Breakfast |
| | | Plenary I Caflich | Plenary II Brown | Plenary IV Jauho | Talks 9 nanoHUB | Outcomes |
| | | Talks 1 Growth | Talks 3 Devices | Talks 6 Transport | Coffee | Coffee |
| | | Coffee Break | | | Talks 10 nextnano3 | Wrap up |
| | | Talks 2 Mechanical properties | Talks 4 Materials | Talks 7 Coherence | | Lunch |
| 12:00-13:00 | | Lunch | Lunch | Lunch | Lunch | |
| | | Tour | Plenary III Klimeck | Talks 8 Electro- mechanical | | |
| | | Group Photo | Talks 5 Computation | Study Group | | |
| | | Study Group | Study Group | | | |
| | | Coffee Break | Coffee Break | Coffee Break | | |
| 16:00-17:30 | Check-in | Discussion | Discussion | Discussion | | |
| 18:00-19:30 | Dinner | Dinner | Dinner | Dinner | Dinner | |
| 19:30 - | | | Poster | | | |

Arakawa, Y. T3
Austing, D. T6
Barettin, D. P
Birner, S. T5, T10
Brown, G. PII
Caflich, R. PI
Chrzan, D. T4
Chuang, S. T3
Clarke, E. T3
Guo, H. T6
Houmark, J. P
Huang, H. T1

Jauho, A. PIV
Johnson, H. T2
Klimeck, G. PIII, T9
Korkusinski, M. T5
Kyriakidis, J. T7
Lassen, B. T8
Lew, A. T1
Lew Yan Voon, L. T8
Li, S. T4
Melnik, R. T8
Neophytou, N. P
Niu, X. P

O'Reilly, E.
Park, H. T2
Pedesseau, L. T8
Roy, D. T8
Schirmer, S. T7
Uskov, A. T7
Vasileska, D. T6
Wang, L. T5
Willatzen, M. T8, P
Zhang, Y. T4
Zhou, M. T2

ABSTRACTS

Advances in quantum dots for nanophotonic and quantum information devices

Yasuhiko Arakawa

Institute for Nano Quantum Information Electronics, The University of Tokyo
arakawa@iis.u-tokyo.ac.jp

The concept of quantum dots for application to semiconductor lasers was proposed in 1982 together with theoretical prediction of temperature insensitive threshold current and high magnetic field experiment [1]. Discovery of formation of a three dimensional small structure in lattice mismatched InAs/GaAs in 1985 triggered the effort to fabricate self-assembled quantum dots [2], which was led to demonstration of quantum dot lasers in the middle of 1990's. Recent remarkable progress in the p-doped layers which increase optical gain and differential gain has realized 1.3- μm p-doped quantum-dot lasers with temperature-insensitive eye-opening under 10-Gb/s modulation without current adjustments between 20 and 70°C [3]. This successful result has brought launch of a curve-out type of venture company, *QD Lasers Corporation* in 2006. In the near future low-cost quantum dot laser modules on GaAs substrates will be brought in telecom commercial market. Recently we have found Si-mediated quantum dots are essentially useful for increasing density of quantum dots and obtaining longer wavelength emission, particularly in MOCVD growth. This result is promising for high performance quantum dot lasers. In addition, we have realized photonic crystal nanocavity quantum dot lasers with the lowest threshold by optical excitation[4]. A concept of single artificial atom lasers will be also briefly discussed.

Quantum dots are also promising to control single photons or entangled photon pairs for quantum information technologies such as quantum cryptography. Recently, we succeeded in demonstrating single photon emission of single-photon pulses in the C-band (1.55- μm band: the highest transmittance in optical telecommunication bands) from a single quantum dot[5]. Furthermore, for realizing high temperature operation, we have demonstrated growth of high-quality GaN/AlN quantum dots with a large binding energy of biexcitons. We achieved triggered single-photon emission at temperatures up to 200 K, a temperature easily reachable with thermo-electric cooling[6]. Moreover, we succeeded in AlN air-bridge photonic crystal nanocavities with GaN quantum dots and have exhibited a quality-factor up to 2,400 which is the highest value in UV region [7].

References

1. Y. Arakawa and H. Sakaki: *Appl. Phys. Lett.*, 40, 939 (1982)
2. L. Goldstein, F. Glas, J. Y. Marzin, M. N. Charasse, and G. Le Roux, *Appl. Phys. Lett.* 47, 1099 (1985)
3. K. Otsubo, N. Hatori, M. Ishida, S. Okumura, T. Akiyama, Y. Nakata, H. Ebe, M. Sugawara and Y. Arakawa
4. M. Nomura, S. Iwamoto, Y. Arakawa *et al.* *Opt. Express* 14, 6308 (2006).
5. K. Takemoto, Y. Sakuma, S. Hirose, T. Usuki, N. Yokoyama, T. Miyazawa, M. Takatsu, and Y. Arakawa, *Jpn. J. Appl. Phys.* 43, 7B, L993, (2004)..
6. S. Kako, C. Santori, K. Hoshino, S. Goetzinger, Y. Yamamoto, Y. Arakawa, *Nature Material*, 5, 887 (2006)
7. M. Arita, S. Ishida, S. Kako, S. Iwamoto, Y. Arakawa, *Applied Physics Letters* (in press)

A vertical quantum dot molecule coherent energy level mixer

D. G. Austing [1,2,*], C. Payette [1,2], G. Yu [1], J. A. Gupta [1], S. V. Nair [3],
B. Partoens [4], S. Amaha [5], S. Tarucha [5,6]

[1] National Research Council of Canada, Institute for Microstructural Sciences M50, Montreal Road, Ottawa, Ontario, K1A 0R6, Canada

[2] McGill University, Department of Physics, Ernest Rutherford Physics Building, 3600 rue University, Montreal, Quebec, H3A 2T8, Canada

[3] University of Toronto, Center for Nanotechnology, 170 College St., Toronto, Ontario, M5S 3E4, Canada

[4] Departement Fysica, Universiteit Antwerpen, Groenenborgerlaan 171, B-2020 Antwerpen, Belgium

[5] ICORP Quantum Spin Project, JST, 3-1, Morinosato, Wakamiya, Atsugi, Kanagawa 243-0198, Japan

[6] Department of Applied Physics, University of Tokyo, 7-3-1, Hongo, Bunkyo-ku, Tokyo 113-8656, Japan

*Corresponding Author: Phone: +1-613-991-9989; FAX: +1-613-990-0202,
E-mail: guy.austing@nrc-cnrc.gc.ca

We observe striking and unexpected magnetic-field induced intra-dot level mixing and quantum superposition phenomena between two, three and four approaching single-particle states in a quantum dot probed by the ground state (“filter”) of an adjacent weakly coupled quantum dot by single-electron elastic resonant tunneling transport measurements. The mixing is attributed to higher order non-negligible anisotropic and anharmonic terms, often neglected, in the confining potential of realistic dots. Pronounced anti-crossing and bright current resonance-to-dark current resonance inter-conversion is observed. For three converging levels, the shape of the crossing region is restricted to four basic types depending on how many (0-, 1-, 2- or 3-) of the couplings between pairs of the constituent states are dominant. The position and strength of the resonances can be modeled within a simple coherent level mixing picture which also allows for the extraction of the eigenvector components. For two-dominant-type three-level-crossing, superposition can lead to complete cancellation of an otherwise strong resonance, an effect which bears a strong resemblance with the quantum optics phenomenon of coherent population trapping in a three-level-“ Λ ” system.

Our quantum dot energy level mixer can help shed light on the microscopic form of the confinement potential in realistic quantum dots often assumed to be highly symmetric in form, and address issues related to coherent and sequential tunneling. Furthermore, we can measure and model quantum superposition effects including current enhancement, suppression and cancellation effects for quantum systems of two or more interacting levels. We focused on three-level mixing and observed the electrical analogue of coherent population trapping.

Electromechanical fields in GaN/AlN Wurtzite Quantum Dots

D. Baretin, B. Lassen, and M. Willatzen

The Mads Clausen Institute for Product Innovation, The University of Southern Denmark
Alsion 2, Dk - 6400 Sønderborg, Denmark

September 26, 2007

GaN/AlN quantum dot (QD) structures have recently received much attention due to their relevance for optoelectronic devices [1]. An important aspect in this context is the influence of the electromechanical-field interactions. We present results of the combined influence of lattice mismatch, piezoelectric effects and spontaneous polarization for wurtzite (WZ) structures consisting of a GaN quantum dot embedded in a AlN matrix [2].

We show that the governing equations for the electromechanical fields are axisymmetric, hence the displacement and electric field solutions are axisymmetric as well, and the original three-dimensional problem can be solved as a two-dimensional mathematical-model problem [3]. We impose Dirichlet boundary conditions far away from the QD, as the displacement vector goes to zero far away from the QD in the case of an infinite matrix.

A quantitative comparison is carried out for four different cases: (1) including lattice mismatch, piezoelectric effects and spontaneous polarization, (2) including lattice mismatch and piezoelectric effects, (3) including only lattice mismatch, and finally (4) including piezoelectric effects and spontaneous polarization. Results are also compared with analytical solutions in the one-dimensional case [4].

We verify that inversion asymmetry in cases (1,2,4) implies field distributions which do not satisfy the $z \rightarrow -z$ symmetry.

References

- [1] Joachim Piprek, *Nitride Semiconductor Devices - Principles and Simulation*, Wiley VHC, 2007.
- [2] Vladimir A. Fonoberov and Alexander A. Balandin. *Journal of Applied Physics*, 94(11):7178-7186, 2003.
- [3] Adel S. Saada, *Elasticity - Theory and Applications*, Pergamon Press Inc. New York, 1974.

- [4] M. Willatzen, B. Lassen, L.C. Lew Yan Voon, and R.V.N. Melnik. *Journal of Applied Physics* 100, 024302, 2006.

Modeling of semiconductor / electrolyte nanostructures with nextnano³

Stefan Birner

*Walter Schottky Institute and Physics Department, Technical University of Munich,
Am Coulombwall 3, D-85748 Garching, Germany*

The quickly progressing technology of low-dimensional semiconductor nanostructures requires and depends on reliable predictive theoretical methods for systematically improving, designing and understanding the electronic and optical properties of such structures. The situation becomes even more complicated if these nanostructures are combined with biomaterials to form bio-sensors [1]. These sensors are gaining importance due to their large potential in commercial applications, like pH, protein, virus or DNA sensors (bio-chips). Ion-selective field effect transistors (ISFETs) usually contain biomaterials in an electrolyte and consist of a two-dimensional electron (or hole) gas (2DEG) in the semiconductor region where a source-drain voltage is applied in the 2DEG plane. The measured source-drain current depends on the electron density in the 2DEG. The goal is to influence the electron density in the 2DEG through a change in the electrostatic potential by the charge distribution inside the electrolyte and at the semiconductor device / electrolyte interface in a reproducible manner, i.e. the electrolyte acts as a gate. Several variations of this concept are possible, e.g. instead of having a 2DEG one could use a nanowire with quantum confinement in two directions, or one could use an optical device where the electrostatic potential in the electrolyte modifies transition energies in quantum wells, quantum wires or even quantum dots. Here, we present theoretical concepts that are necessary for realistically modeling the electrolyte solution, its interaction with the semiconductor device surface, and the semiconductor device itself. These models have to be solved self-consistently.

An electrolyte is an aqueous solution containing dissolved ions (e.g. Na^+ , Cl^-) that result from the dissociation of salts. Usually, electrolytes that are used as bio-sensors are buffer solutions. A buffer is a solution that resists changes in H_3O^+ and OH^- ion concentrations (and consequently the pH value) upon addition of small amounts of acid or base, or upon dilution. The concentration of the ions that are contained in the buffer depends on the pH value and the pK_a ' value (acid dissociation constant) and can be calculated using the well-known Henderson-Hasselbalch equation. In addition, the pK_a ' value depends on temperature and on ionic strength [2] in a self-consistent way. For instance, when using the phosphate buffer (PBS) the concentrations of the buffer ions at a particular pH value are governed by three different pK_a ' values and thus it is extremely hard to derive the concentrations analytically, but this can be programmed easily in an iterative scheme. We extended this model to allow the variables pH, pK_a ' and ionic strength to vary with spatial coordinate. Such an approach is necessary for analytes that produce local charge variations in the electrolyte, e.g. a charged molecule that binds to the semiconductor device surface. Furthermore, a local variation of pH is critical for the operation of EnFETs (enzyme FETs) where the enzyme reaction depends on the pH value. The distribution of all ion charges in the electrolyte is governed by the Poisson-Boltzmann equation. Very often the Poisson-Boltzmann equation is being linearized yielding the Debye-Hückel approximation. However, such a simplification is generally not applicable in real devices and only valid for special and very limited cases. One of our challenges at present is to include the current equation into the self-consistent cycle because in contrast to MOSFET simulations, where the gate material is usually not included in the transport simulations (the gate voltage enters as a boundary condition and is constant throughout the whole gate region), the electrostatic potential at the semiconductor device / electrolyte interface and inside the electrolyte might vary in a complicated way depending on the charge

carrier distribution in the semiconductor. Electrolytes can be straightforwardly included into any program that solves the Schrödinger, Poisson and current equations self-consistently. Essentially, only the Poisson equation has to be modified by the charge density distribution in the electrolyte and by a suitable sheet charge density at the semiconductor device / electrolyte interface. The charge density inside the electrolyte at position \mathbf{x} is given by

$$\rho(\mathbf{x}) = \sum_{i=1}^n z_i e c_{i,0} \exp\left(-\frac{z_i e (\phi(\mathbf{x}) - U_G)}{k_B T}\right) \quad (1)$$

where z_i is the ion valency, e is the positive elementary charge, $c_{i,0}$ is the bulk concentration of the ion species i , $k_B T$ is the thermal energy at temperature T and U_G is the bulk electrolyte potential (which can be varied by a gate electrode). $\phi(\mathbf{x})$ is the electrostatic potential that is obtained by solving self-consistently the nonlinear Poisson-Boltzmann equation in the overall device, i.e. in both the electrolyte as well as in the semiconductor region

$$\nabla \cdot [\varepsilon_0 \varepsilon(\mathbf{x}) \nabla \phi(\mathbf{x})] = -\rho(\mathbf{x}, \phi) \quad (2)$$

where ε_0 is the permittivity of vacuum and ε is the relative permittivity of either the electrolyte or any of the semiconductor materials. Interface reactions can be taken into account by the so-called site-binding model for amphoteric oxide surfaces [3, 4] where the adsorption or dissociation of H^+ and OH^- ions at oxide / electrolyte interfaces lead to interface charge densities which depend on both, the electrostatic potential at the interface and the pH value of the electrolyte. These interface densities simply have to be included to the charge density ρ in Eq. (2). We included these models into our software package `nextnano3` [5], so that we are now able to model semiconductor / electrolyte systems in one [6], two and three dimensions for arbitrary geometries and material compositions. An example of bio-sensors are silicon nanowires that are surrounded by an electrolyte and the specific charge distribution in the electrolyte may arise from protein binding to the semiconductor surface where the surface is functionalized with a lipid layer so that proteins can specifically bind to the headgroups of the lipids on the surface. The self-consistent calculation of the spatial charge and potential distribution for different ion concentrations in the electrolyte can be used to interpret experimental data and to optimize the sensitivity of these devices. Modeling of these structures is also essential in order to interpret capacitance-voltage data (Mott-Schottky analysis) correctly. A highly promising material system for bio-sensors are nitride-based devices (e.g. AlGaN/GaN) because they are not toxic (in comparison to GaAs-based ion sensors), possess a chemically inert oxide surface and they are extremely sensitive to changes of the surface charge or surface potential due to their large built-in piezo- and pyroelectric fields. As examples we present one- and two-dimensional simulations of protein, DNA and pH sensors based on different semiconducting materials (silicon, diamond and nitride) and conclude with an outlook on optical bio-sensors based on quantum well and quantum dots.

- [1] *Nanowire Nanosensors for Highly Sensitive and Selective Detection of Biological and Chemical Species*, Y. Cui, Q. Wei, H. Park, C. M. Lieber, *Science* **293**, 1289 (2001)
- [2] *Buffer solutions: The basics*, R. J. Beynon, J. S. Easterby, Oxford University Press (1996)
- [3] *Development of an ion-sensitive solid-state device for neurophysiological measurements*, P. Bergveld, *IEEE Trans. Biomed. Eng.* **17**, 70 (1970)
- [4] *Ionizable surface group models of aqueous interfaces*, T. W. Healy, L. R. White, *Adv. Colloid Interface Sci.* **9**, 303 (1978)
- [5] The `nextnano3` software can be obtained from <http://www.wsi.tum.de/nextnano3> and <http://www.nextnano.de>.
- [6] *Theoretical study of electrolyte gate AlGaIn/GaN field effect transistors*, M. Bayer, C. Uhl, P. Vogl, *J. Appl. Phys.* **97**, 033703 (2005)

“Nanostructured Materials for Electronic and Optical Applications”

Gail J. Brown

Air Force Research Laboratory

Materials & Manufacturing Directorate

There are a variety of low dimensional materials that will play a role in the development of optoelectronic and electronic devices. These nanostructured materials range from semiconductor heterostructures to novel carbon structures to metallic nanoparticles. The underlying physics may depend on quantum confinement effects of electrons in a dot or a surface plasmon resonance, or other unique property changes that occur at the nanoscale. There are also a variety of growth and processing techniques employed to create these materials. For instance semiconductor quantum dots can be grown by molecular beam epitaxy, solution growth or reverse micelles in carbon dioxide. Often new materials are produced faster than we can identify or model their properties or potential applications. Computational modeling of these nanoscale materials is essential to material selection and optimization for a given application. An overview of some key low dimensional materials under study for electronic and optical devices will be presented. Some examples of what has been accomplished in quantum confined semiconductors will be given, such as quantum wells and superlattices for infrared detection. The benefits of combining theorists and experimentalists on the same team will be highlighted.

Modeling and Simulation for Epitaxial Growth and Pattern Formation

Russel Caffisch *

Abstract

Growth of an epitaxial thin film involves physics on both atomistic and continuum length scales. For example, diffusion of adatoms can be coarse-grained, but nucleation of new islands and breakup for existing islands are best described atomistically. The lattice properties of the film are determined by those of the underlying substrate. In heteroepitaxial growth, e.g., Germanium on Silicon, mismatch between the lattice spacing of the Silicon substrate and the Germanium film introduces strain into the film, which can significantly influence the material structure, leading for example to the formation of quantum dots. Technological applications of quantum dot arrays require a degree of geometric uniformity that has been difficult to achieve. One approach to overcoming this difficulty is to prepattern the system, for example with buried dislocation lines. This talk will describe mathematical modeling, simulation methods and computational results for epitaxial growth, strain in thin films and pattern formation. The growth simulations use an island dynamics model with a level set simulation method. Strain computations can be computationally intensive, so that effective simulation of atomistic strain effects relies on an accelerated method that incorporates algebraic multigrid and an artificial boundary condition. Simulations that combine growth and strain will be presented showing spontaneous and directed self-assembly of patterns (quantum dots and wires) on thin films.

*Mathematics Department, University of California at Los Angeles, Los Angeles, CA 90095 USA

Modeling the Synthesis and Thermodynamic Properties of Ge Nanocrystals Embedded in Amorphous Silica

Daryl C. Chrzan, Department of Materials Science and Engineering, University of California, Berkeley, CA, 94720, USA and Materials Sciences Division, Lawrence Berkeley National Laboratory, Berkeley, CA, 94720, USA

The ion beam synthesis (IBS) of Ge nanocrystals embedded in amorphous silica is a two step process. In the first step, 50-150 keV Ge ions are implanted within a silica substrate using an ion accelerator. In the second step, the sample is annealed. Typical ion doses fall in the $4 \times 10^{16} \text{ cm}^{-2}$ range. Typical annealing conditions are 950 C for 1 hour. The resulting Ge nanocrystals are found within a band roughly 100 nm thick, buried roughly 50 nm below the surface of the silica. A subsequent HF etch can be used to liberate the nanocrystals from the matrix.

The Ge nanocrystals embedded in silica offer an unusual opportunity for detailed characterization. Nanocrystal size distributions can be determined using both transmission electron microscopy (TEM) and atomic force microscopy (AFM). The stress state within the nanocrystals can be measured using Raman spectroscopy. Further, the thermodynamics of the nanocrystals can be studied using *in situ* TEM heating. In contrast to free-standing nanocrystals, confined nanocrystals offer an ideal laboratory to study both the melting *and* solidification of the nanocrystals, and thus allow a more complete model of the phase transition to be developed.

Experimental studies of the Ge nanocrystals confined in silica have revealed much interesting behavior. First and foremost, the as synthesized nanocrystals are under compressive stresses. Subsequent thermal annealing serves to relieve this stress. Further, measured nanocrystal size distributions are inconsistent with those expected from traditional coarsening models. Finally, *in situ* TEM melting/solidification experiments reveal a large melting point hysteresis (approximately 470 K) nearly centered on the bulk melting point of Ge. Thus the confined nanocrystals melt at a temperature well *above* the bulk melting point of Ge. This observed increase is surprising, particularly in light of the fact that the amorphous silica matrix cannot lead to the lattice registry effects typically thought to be the origin of increased melting points for confined nanocrystals.

We have developed a model for the nucleation and growth via IBS of Ge nanocrystals embedd in silica. The model relies on both kinetic Monte Carlo simulations of the growth process, and a complementary approach involving the integration of a set of coupled rate equations. When coupled with appropriate experiments, these tools provide substantial insight into the nucleation and growth process. For example, the measured shapes of the Ge nanocrystal size distributions can only be obtained if the Ge clusters nucleate during the implantation, and then are modified by the damage arising from the implantation. The damage is so severe that the Ge clusters are in an amorphous state. Upon annealing, the clusters melt and coarsen (though not rapidly) in a liquid state. Cooling then leads to crystallization of the nanocrystals.

The large hysteresis in the melting point of the confined nanocrystals was also modeled. The model, which employs classical nucleation theory and reflects properly the geometry of

the confined nanocrystals, correctly predicts the observed melting point behavior without the need to invoke lattice registry effects. Within this model, the melting point hysteresis arises because the liquid-Ge/silica interface energy is nearly equal to the solid-Ge/silica interface energy, and of the right magnitude to require nucleation for *both* the melting and solidification transitions.

This work is supported by the Director, Office of Science, Office of Basic Energy Sciences, Division of Materials Science and Engineering of the U. S. Department of Energy under Contract No. DE-AC02-05CH11231.

Modeling of Optical Gain and Chirp of Quantum-Dot Lasers and Comparison with Experiment

Shun Lien Chuang
Department of Electrical and Computer Engineering
University of Illinois at Urbana-Champaign
1406 West Green Street
Urbana, Illinois 61801, USA
Tel: 217-333-3359, Fax: 217-333-5701, Email: s-chuang@uiuc.edu

We discuss our theoretical model of strained quantum-dot lasers including the band structure, the optical gain spectrum, the refractive index change, and the chirp. We take into account the homogeneous and inhomogeneous broadening of the optical transitions in the quantum-dot laser structures. We use a Gaussian function for the optical gain spectrum and the corresponding confluent geometrical function for the change in refractive-index spectrum, both of which satisfy the Kramers-Kronig relations. We then performed experiments to measure the optical gain, refractive index change, and the chirp spectra as a function of the injection current in order to confirm our theoretical model. We compared continuous wave (cw) measurements with pulsed measurements of the quantum-dot lasers to illustrate the influence of the thermal effects. It is shown that our theoretical model for the optical gain and chirp spectra gives good agreement with the experimental data, when lasers are under pulsed measurements so the thermal effects are minimized. We demonstrate that quantum dot lasers have low chirp, as expected from theory. With the introduction of p-type doping into the quantum dots, our model indicates improved gain and reduced chirp performance of the p-doped quantum-dot lasers compared with undoped samples.

References:

1. J. Kim, H. Su, S. Minin, and S. L. Chuang, "Comparison of linewidth enhancement factor between p-doped and undoped quantum-dot lasers," *IEEE Photon. Technol. Lett.*, vol. 18, pp. 1022-1024, 2006.
2. J. Kim and S. L. Chuang, "Theoretical and experimental study of optical gain, refractive index change, and linewidth enhancement factor of p-doped quantum-dot lasers," *IEEE J. Quantum Electron.*, vol. 42, pp. 942-952, 2006.

InAs/GaAs Quantum Dot Bilayers: Nanoscale Strain Engineering

Edmund Clarke, Patrick Howe, Peter Spencer, Edmund Harbord, Ray Murray
Imperial College London, U.K.

Email: edmund.clarke@imperial.ac.uk

In addition to novel optical properties arising from their discrete density of states, InAs/GaAs quantum dots (QDs) have attracted interest for device applications since they offer the possibility of long wavelength optoelectronic devices based on GaAs. InAs/GaAs QD devices operating at 1300 nm are now well established but extension of the QD emission wavelength towards the 1550 nm telecoms window is rarely reported.

One method to extend the emission wavelength of InAs/GaAs QDs is to exploit the growth conditions that occur when two QD layers are closely stacked. Strain from the underlying (seed) layer affects the growth of the second layer, with preferential QD nucleation above buried QDs. The seed layer acts as a template for growth of the second layer and growth conditions can then be modified, particularly by reducing the growth temperature, in order to obtain QDs with long emission wavelengths but with the QD density determined by the seed layer [1, 2]. Room temperature emission and lasing beyond 1300 nm is demonstrated by these bilayers [3], without the use of InGaAs capping or dots-in-a-well (DWELL) growth techniques. By capping the second QD layer with InGaAs, further extension of the emission wavelength is achieved, to 1515 nm at room temperature, with a narrow linewidth of 22 meV (figure 1).

This talk outlines both the growth and the resultant optical properties of this novel QD system. In addition to the long emission wavelengths that can be achieved from these QDs, exceptionally narrow luminescence linewidths are obtained (<12 meV at 10 K) and efficient electronic coupling between the QD layers leads to suppression of emission from the seed layer.

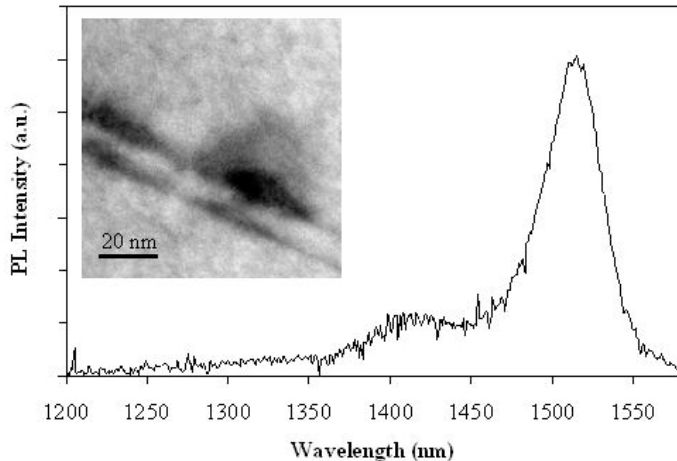


Figure 1: Room temperature photoluminescence spectrum obtained from an InGaAs-capped InAs/GaAs QD bilayer sample. Inset: Cross-sectional transmission electron microscope image of InGaAs capped QD bilayer (Image courtesy S. Kadkhodazadeh, Imperial College).

Lasers incorporating QD bilayers demonstrate characteristics specific to QD lasers, including simultaneous lasing in the ground state and first excited state of the QDs (not the seed layer) [4]. A comparison of optical spectroscopy and electrical derivative measurements [3, 5] (figure 2), shows that there is only partial clamping of the junction voltage above the laser threshold in QD lasers, in contrast to bulk and quantum well lasers. Quenching of the ground state lasing at high currents is also observed, which cannot easily be explained by models for dual state lasing involving carrier relaxation bottlenecks [4].

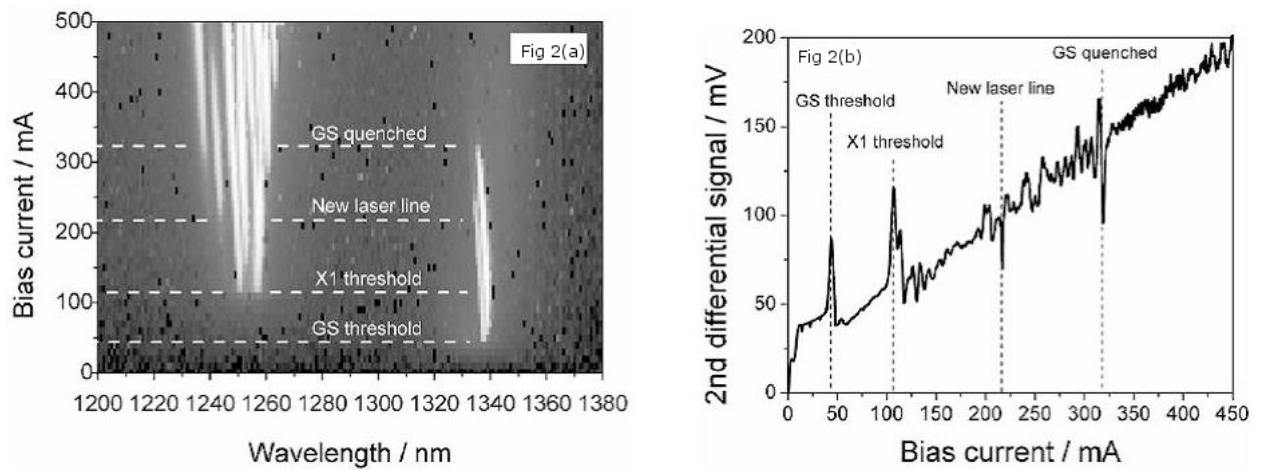


Figure 2: (a) Optical spectra of InAs/GaAs QD bilayer laser with increasing current, (b) corresponding electrical derivative measurement.

1. E. C. Le Ru, P. Howe, T. S. Jones, R. Murray, Phys Rev B **67**, 165303 (2003)
2. P. Howe, E. C. Le Ru, E. Clarke, B. Abbey, R. Murray, T. S. Jones, J Appl Phys **95**, 2998 (2004)
3. P. Spencer, E. Clarke, P. Howe, R. Murray, Electron Lett **43**, 574 (2007)
4. A. Markus, M. Rossetti, V. Calligari, D. Chek-Al-Kar, J. X. Chen, A. Fiore, R. Scollo, J Appl Phys **100**, 113104 (2006)
5. T. L. Paoli, IEEE Trans Electron Dev **23**, 1333 (1976)

Mesoscopic Spin-Hall Effect

Hong Guo

Center for the Physics of Materials and
Department of Physics,
McGill University, Montreal, PQ, Canada H3A 2T8.

For a pure semiconductor with spin-orbital (SO) interactions, recent literature [1] has proposed that a dc electric field in one direction, say z direction, can induce a flow of spin-current in x-direction: such a spin-current is dissipation-less because the external electric field does no work to the electrons flowing inside the spin-current. For a mesoscopic sample, the flow of spin-current induces a mesoscopic spin-Hall effect that survives weak disorder. In this talk, I will describe the physics of mesoscopic spin-Hall phenomenon induced by SO interaction [2], reporting a universal spin-Hall conductance fluctuation [3], and summarising the physics of mesoscopic spin-Hall effect in a low field phase diagram [4]. The numerical technique for efficiently solving the 2D quantum scattering problem will also be presented.

[1] S. Murakami et al, Science 301, 1348 (2003).

[2] Q.F. Sun, J. Wang and Hong Guo, Phys. Rev. B 71, 165310 (2005).

[3] W. Ren et al, Phys. Rev. Lett. 97, 066603 (2006).

[4] Z. Qiao et al, Phys. Rev. Lett. 98, 196402 (2007).

Influence of Coulomb interactions on quantum coherence in quantum dots

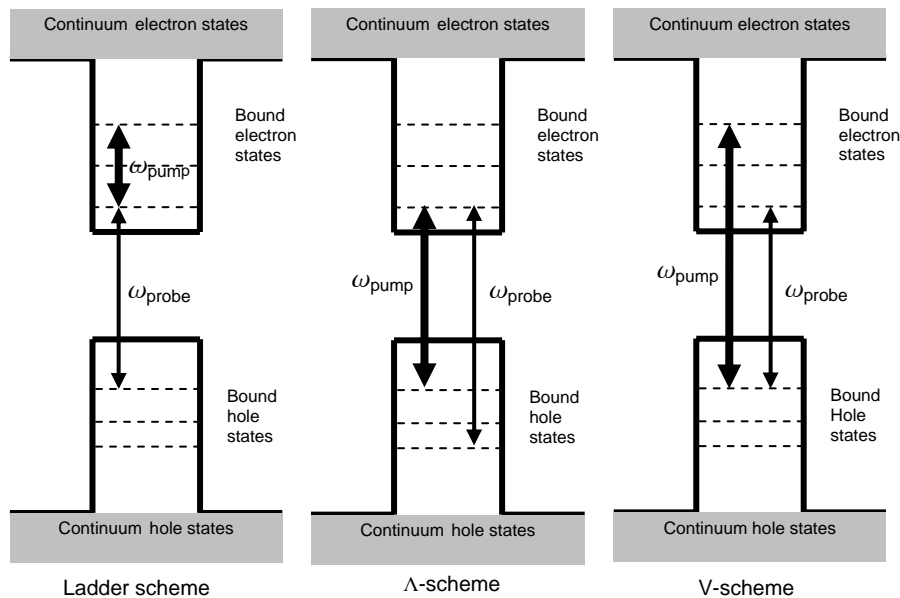
Jakob Houmark-Nielsen¹, Antti-Pekka Jauho¹, Torben R. Nielsen² and Jesper Mørk²

¹⁾ MIC-DTU, Technical University of Copenhagen

²⁾ COM-DTU, Technical University of Copenhagen

Demonstrations of exotic quantum coherence effects in atomic gases such as electromagnetically induced transparency¹ (EIT) and slow light², has spurred a large interest in extending these results to semiconductor nanostructures. A major motivational factor lies in the application for optoelectronic devices; for instance an all optical buffer³ based on slow light in quantum dots has been proposed. Most theoretical approaches has taken offset in the atomic description, thus treating the semiconductor as an inhomogeneously broadened three-level system, with strong dephasing effects, thereby disregarding many-particle effects. A physically more realistic model would take into account other quantum dot states, as well as the continuum of states generated by the quantum well embedding the dots. Furthermore, the Coulomb interaction that serves to couple discrete and continuum states, redistribute carriers and renormalize energies and fields, should be taken into account. Recent publications^{4,5} has addressed these issues, however the treatment is done in the transient regime and for application purposes the steady-state properties are of particular interest.

We compare steady-state calculations for various EIT schemes in a system comprised of InAs quantum dots embedded in a GaAs quantum well, using a many-body model incorporating Coulomb effects on the Hartree-Fock level.



¹S. E. Harris, J. E. Field, and A. Imamoglu, Phys. Rev. Lett. **64**, 1107 (1990).

²L. V. Hau, S. E. Harris, Z. Dutton, and C. H. Behroozi, Nature **397**, 594 (1999).

³C. J. Chang-Hasnain, P. C. Ku, J. Kim, and S. L. Chuang, Proc. IEEE **91**, 1884 (2003).

⁴W. W. Chow, H. C. Schneider, and M. C. Phillips, Phys. Rev. A **68**, 053802 (2003).

⁵S. Michael, W. W. Chow and H. C. Schneider, App. Phys. Lett. **89**, 181114 (2006).

Predictive Modeling of Nanorods Synthesis

Hanchen Huang

Department of Mechanical, Aerospace and Nuclear Engineering
Rensselaer Polytechnic Institute (<http://www.rpi.edu/~huangh>)

Modeling has been prevalent, and predictive modeling is a challenge. For modeling to be predictive, it is more critical to be physics-based than to appear multiscale, although the two do not necessarily contradict each other. This presentation shows one example of predictive modeling - self-organized bifurcation during nanorods synthesis. The presentation consists of four elements: (1) discovery of a surface diffusion barrier, (2) conceptual design through integration of the discovery and existing knowledge, (3) test of concept using atomistic simulations, and (4) experimental validation.

The discovery is a substantially large diffusion barrier on surface. An atom usually experiences a diffusion barrier on a flat surface. When the atom diffuses down a monolayer step, there is an additional barrier, the Ehrlich-Schwoebel (ES) barrier. As the step thickness is more than one monolayer, the diffusion barrier increases substantially. For Cu, the diffusion barrier of an atom is 0.08 eV on a flat surface, 0.16 eV down a monolayer step, and 0.40 eV down a multilayer step [1]; the 0.40 eV is referred to as 3D ES barrier. Based on these diffusion barriers, kinetic Monte Carlo simulations show that facet dimension during typical physical vapor deposition is on the order of 300 nm, comparable to the experimental value of 200 nm. In contrast, without the barrier of 0.40 eV, modeling would estimate the facet dimension to be about 100,000 nm, three orders of magnitude different from the experimental value.

Integration of the 3D ES barrier with two other pieces of existing knowledge leads to a conceptual design of nano-synthesis [2]. These two pieces are geometrical shadowing and stacking fault. Using glancing angle deposition and thereby geometrical shadowing, Robbie and Brett [3] have demonstrated the growth of nanorods. It is common that introductory materials textbooks will cover the stacking fault formation during growth of face-centered-cubic (FCC) crystals. The conceptual design starts with a $\langle 110 \rangle$ Cu nanorod (or another FCC material), as shown in Figure 1a. Due to geometrical shadowing, deposited atoms land primarily on top of the nanorods. The 3D ES barrier prevents the deposited atoms from diffusing down. As deposition continues, atoms may occupy stacking fault positions (indicated by red spheres in Figure 1b). The intersection of the two stacking fault layers is a high energy $\Sigma 9$ grain boundary. Atoms do not prefer the

high energy site and stay away from the grain boundary. Bifurcation occurs, as shown in Figure 1c. Continued deposition leads to further growth. Again, the 3D ES barrier and the geometrical shadowing keep atoms on top of the branched nanorods, as shown in Figure 1d.

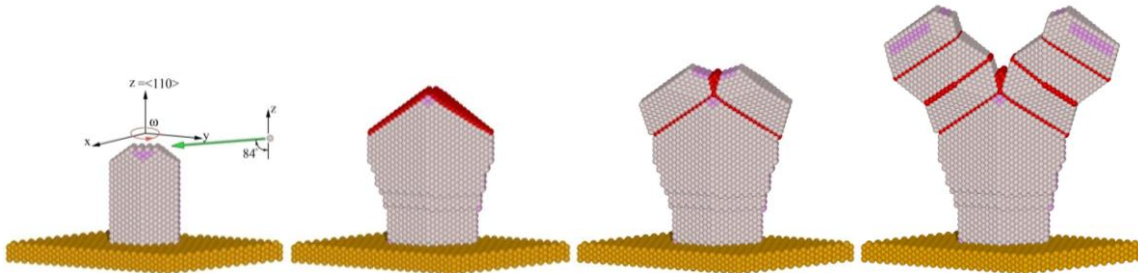


Figure 1: Conceptual design of nanorod bifurcation: (a) to (d) from left to right.

Next, classical molecular dynamics simulations show that the conceptual design is feasible. Up to this point, the self-organized bifurcation of nanorods (or the formation of Y-shaped nanorods) remains a model prediction. A subsequent magnetron sputtering deposition experiment has provided the validation. As shown in Figure 2, the self-organized bifurcation indeed occurs as predicted.

It is worth to mention that the self-organized bifurcation should be a generic feature of low-stacking-fault-energy FCC materials and possibly diamond cubic materials.

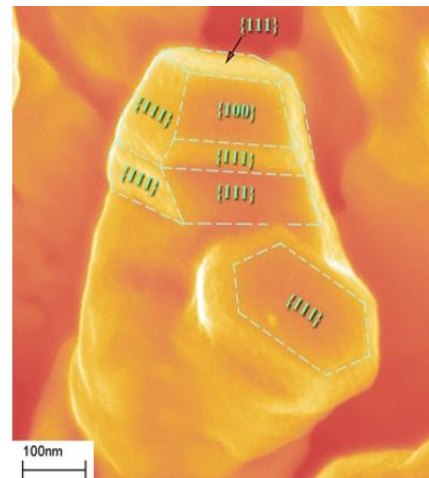


Figure 2: SEM image of Cu.

References:

1. S. J. Liu, Hanchen Huang, and C. H. Woo, **Applied Physics Letters** **80**, 3295-3297 (2002).
2. J. Wang, Hanchen Huang, S. V. Kesapragada, and D. Gall, **Nano Letters** **5**, 2505-2508 (2005).
3. K. Robbie and M. J. Brett, **Journal of Vacuum Science and Technology A** **15**, 1460-1465 (1997).

Electronic transport through Si nanowires: role of bulk and surface disorder, and implications to localization*

Antti-Pekka Jauho

*MIC - Department of Micro- and Nanotechnology, NanoDTU,
Technical University of Denmark, DK-2800 Kgs. Lyngby, Denmark
Laboratory of Physics, Helsinki University of Technology, 2150 Espoo, Finland*

The theoretical scientist attempting to model transport in modern nanoscale systems faces many challenges. The number of atoms requiring a microscopic treatment may vary from a few to several millions. The transport may be coherent, or dominated by interaction effects. In this talk I describe a number of ways to attack this problem; the common denominator is that we wish to study the physics of Si-nanowires of realistic size, disorder, and dopants [1]. Specifically, in the first part of this talk I describe two different numerical approaches (a real-space Kubo formula, and the recursive Green's function technique) to calculate the resistance and mean free path in long metallic and semiconducting silicon nanowires. We use density functional theory to find relaxed atomic structures, without using adjustable parameters. Two specific models of disorder are considered: unpassivated, surface reconstructed SiNW's are perturbed by random on-site disorder, whereas defects in hydrogen passivated wires are introduced by randomly removed H atoms. Next, I combine the ideas of scaling theory and universal conductance fluctuations with density-functional theory to analyze the statistical aspects of the conduction properties of doped silicon nanowires [2]. Specifically, we study the cross-over from ballistic to diffusive transport in B or P doped Si-nanowires by computing the sample averaged conductance $\langle G \rangle$, and sample-to-sample variations $\text{std}(G)$ as a function of energy, doping density, wire length, and the radial dopant profile. Our main findings are: (i) the main trends can be understood based on the scattering properties of single dopants; (ii) the sample-to-sample fluctuations depend on energy but not on doping density, thereby displaying a degree of universality, and (iii) in the diffusive regime the analytical predictions of the DMPK theory are in good agreement with our ab initio calculations.

-
- [1] T. Markussen, R. Rurali, M. Brandbyge, and A. P. Jauho, Phys. Rev. B **74**, 245313 (2006).
 - [2] T. Markussen, R. Rurali, A. P. Jauho, and M. Brandbyge, Phys. Rev. Lett. **99**, 076803 (2007).

* Work done in collaboration with Troels Markussen, Riccardo Rurali, and Mads Brandbyge.

Modeling dislocation effects on electronic and optical properties in III-V semiconductors

Harley T. Johnson, Jeong Ho You, and Jun-Qiang Lu
Department of Mechanical Science & Engineering
University of Illinois at Urbana-Champaign, Urbana, IL 61801 USA

The presence of dislocations in semiconductor thin films and quantum dots is undesirable from the perspective of electronic and optoelectronic device applications. A dislocation takes on a charge when free electrons are trapped at dangling bonds along the core, and the strain field of a dislocation leads to band bending in the region near the core. These effects are sources of scattering that typically reduces electron mobility in films with high dislocation densities. Reductions in photoluminescence intensity with increasing dislocation density are also observed, although the effects are very different among various group III-V semiconductor alloys. Some materials, like GaAs, have severely degraded photoluminescence intensity in the presence of even low dislocation densities. Other materials, like GaN, have a robust optical response when the dislocation density is many orders of magnitude larger, although the dislocations are viewed as a possible source of luminescence at energies within the bandgap.

In this work, a computational framework is presented for studying the effects of dislocations on both electrical and optical properties in these materials. Dislocations are first studied using ab initio atomistic methods in order to determine the chemistry and electronic structure of the core. Then the dislocation effect at the continuum scale is treated using classical electrostatics, whereby a screened potential is assigned to mimic the effect of the dangling bonds along the dislocation line, and a deformation potential is assigned to model the electrostatic effect of the strain field. Optical properties are then studied using a multi-band effective mass model to compute the electron and hole energy levels, the density of states, and ultimately the optical emission spectra of a material containing a prescribed density of dislocations, as a function of both temperature and free carrier concentration. Electron mobility is computed separately by means of a classical scattering model incorporating the dislocation electrostatic potential.

A wide range of experimental results are then predicted and interpreted based on the computational model, especially for the interesting case of GaN. The reduction in photoluminescence intensity as a function of both edge and screw dislocation density is accurately predicted for wurtzite GaN. Also, the possibility of yellow luminescence in GaN arising from oxygen impurities along edge dislocation cores is established. The experimentally observed effect of dislocation density on electron drift and Hall mobility in GaN films with low free carrier concentration is explained. Finally, the long-studied disparity in the dislocation sensitivity between GaN and GaAs is considered in the context of this new model.

References:

Jeong Ho You, Jun-Qiang Lu and H. T. Johnson, "Electron scattering due to threading edge dislocations in epitaxial wurtzite GaN," *Journal of Applied Physics*, **99**, 033706 (2006).

Jeong Ho You and H. T. Johnson, "Effect of threading edge dislocations on the photoluminescence spectrum in n-type wurtzite GaN," *Physical Review B*, **76**, 115336 (2007).

Jeong Ho You and H. T. Johnson, "Effect of screw dislocation density on optical properties in n-type wurtzite GaN," *Journal of Applied Physics*, **101**, 023516 (2007).

Multi-Million Atom Simulations with NEMO 3-D and its Deployment on nanoHUB.org

Gerhard Klimeck

*School of Electrical and Computer Engineering,
Network for Computational Nanotechnology, Purdue University,
West Lafayette, IN-47907, USA.*

Novel nanoelectronic devices such as quantum dots, nanowires, and ultra-scaled quantum wells are expected to significantly enhance existing nanoelectronic technologies. The behavior of carriers and their interaction with their environment need to be fundamentally explained at a quantum mechanical level. Modeling efforts that are targeted to enhance the theoretical understanding of these devices are underway worldwide. Most of these device level descriptions utilize an effective mass approach. However, the concepts of device and material meet at the nanometer scale. The new device is really a new material and vice versa. A representation of the constituent materials at the atomic resolution is needed to quantitatively model devices with a countable number of atoms. While atomistic representations are novel to device physicists, the concept of finite devices that are not infinitely periodic is novel in the semiconductor materials modeling community. The 3-D Nanoelectronic Modeling Tool (NEMO 3-D) is an electronic structure simulation code for the analysis of quantum dots, quantum wells, nanowires, and impurities. NEMO 3-D uses the Valence Force Field (VFF) method for strain and the empirical tight binding (ETB) for the electronic structure calculations. Various ETB models are available, ranging from single s orbitals (single band effective mass), over sp^3s^* to $sp^3d^5s^*$ models, with and without explicit representation of spin. The code is highly optimized for operation on cluster computing systems. Simulations of systems of 64 million atoms (strain) and 52 million atoms (electronic structure) have been demonstrated. The code is efficiently parallelized and typically executed on around 32 CPUs. It has, however, also been demonstrated to scale well to up to 8,192 processors on two of today's most advanced parallel machines.

To truly have impact on the research, experimental, and educational efforts of the community, relevant tools must be put into the hands of experimentalists and educators. NEMO 3-D offers the opportunity to engage both educators and advanced researchers, utilizing a single code. NEMO 3-D has been released as open source. An educational version of NEMO 3-D has been released on the nanoHUB and user-friendly versions that enable large-scale parallel executions are under development. Over 646 users ran over 4,800 simulations using the educational NEMO 3-D version embodied in the nanoHUB quantum dot lab in the past 12 months.

nanoHUB.org is operated by the Network for Computational Nanotechnology (NCN). The NCN was established as a multi-university initiative to create a community resource for nanoscience and nanotechnology—online services for research, education and collaboration. The NCN's cyberinfrastructure delivers online simulation, courses, tutorials, services for collaboration, and more. The NCN's objective is to put theory, simulation, experimental and computational research, and education together with

cyberinfrastructure in a way that empowers the development of nanotechnology as a new engineering discipline. NCN's central outreach vehicle is the community web site nanoHUB.org.

The nanoHUB provides unique educational resources, collaborative services, and delivers simulation, visualization, and high-performance computing services online *free of charge*. The nanoHUB's signature service is online simulation. The power of simulation is fully realized, when software leaves the domain of the computational experts and is released to users with real problems to solve. Acquisition, installation, and maintenance of software are, however, a barrier to its use — especially in new fields where commercial packages are not available. The NCN's goal is to dramatically lower the barriers to the pervasive use of simulations in research and education. The nanoHUB has been used by over 26,100 users in the 12 months leading to September, 2007. Over 5,900 users have launched over 226,000 simulation in that time frame. The presentation reviews the mission of the NCN exemplified by the development and deployment of the NEMO 3-D tool.

This presentation will overview NEMO 3-D developments, results, and nanoHUB deployment and the presentation will overview the nanoHUB and its impact on the community. This work has been conducted by a large number of people consistent of computational scientists, physicists, electrical engineers, and students at JPL and Purdue as well as the nanoHUB development team at Purdue. This work is supported by the NSF, the Indiana 21st Century Fund, Semiconductor Research Corporation (SRC), and the Army Research Office (ARO).

Atomistic calculations of electronic and optical properties of semiconductor nanostructures

M. Korkusinski¹, W. Sheng^{1,2}, M. Zielinski¹, and P. Hawrylak¹

¹*Quantum Theory Group, Institute for Microstructural Sciences,
National Research Council, Ottawa, Canada K1A0R6*

²*Department of Physics, Fudan University, Shanghai 200433, China*

We present the computational procedure for calculation of the electronic and optical properties of semiconductor self-assembled quantum dots. The procedure starts with the definition of the shape, structure, and material composition of the system on the atomistic level. The mismatch of the lattice constants of the quantum dot and barrier materials causes displacements of atoms from their bulk positions, i.e., the strain field. We find the optimal atomic positions by minimizing the total elastic energy of the system using the Valence Force Field model in the first-nearest-neighbor approximation.

Once the equilibrium structure of the sample has been established, we proceed to calculating the single-particle states of the electron and hole confined in the nanostructure using tight-binding approaches. We use two tight-binding models. One of them is the fully atomistic $sp^3d^5s^*$ approach, accounting for the symmetry of the zincblende crystal lattice of the system, but requiring 31 external parameters. The second approach involves the effective bond orbital model (EBOM) defined on only one sublattice of the zincblende crystal. The EBOM model can be extrapolated to the kp method close to the Γ point, and is parametrized by seven material constants, six of which are the kp parameters. In both tight-binding models we account for the external electric field by appropriately modifying the onsite (diagonal) matrix elements, while the magnetic field is treated in EBOM via the Peierls substitution. The single-particle wave functions obtained in this step are used to compute the joint optical density of states of the nanostructure.

Next we consider the system of interacting N electrons and M holes forming neutral or charged excitonic complexes confined in the quantum dot. To calculate the energies and eigenstates of these complexes we use the configuration-interaction method. This method involves (i) creation of all possible configurations of the $N+M$ carriers on the single-particle states, (ii) writing the Hamiltonian matrix in the basis of these configurations, and (iii) numerical diagonalization of this matrix. We calculate the Coulomb scattering matrix elements approximately using the atomistic single-particle wave functions.

In the last step of the procedure we obtain the emission spectra of the confined excitonic complexes by applying the Fermi's Golden Rule to the many-body eigenenergies and wave functions.

We discuss the details of this computational procedure on several model quantum dot systems. First, we compare the single-particle spectra of an InAs/GaAs quantum disk obtained with the atomistic approaches to those obtained by the effective mass and kp methods. We find good correspondence between the four models, which indicates that the properties of the single quantum dot can be understood qualitatively on the effective-mass level. We find, however, that the effective-mass approximation is not sufficient for the vertically coupled double quantum dot molecule. We show that in this system the valence band mixing effects strongly affect the properties of confined holes. In particular,

the symmetry of the molecular states of the hole depends on the distance between disks, so that the ground hole state is antibonding if the disks are sufficiently far apart. While the kp approach is capable of capturing the essential physics of this system, the atomistic treatment is needed to properly resolve the effects of strain and symmetry of the underlying crystal lattice.

In the last example we illustrate the configuration interaction approach by calculating the emission spectra of neutral multiexcitons confined in the single dot. We demonstrate the signatures of hidden symmetries in these spectra.

Decoherence and Relaxation in Strongly Interacting Quantum Dots

Jordan Kyriakidis
Dalhousie University
Halifax, Canada

I'll present theoretical results of our work on quantum dots defined electrostatically in a two-dimensional electron gas. Depending on available time, I'll try to discuss three areas of research:

1) Resonant Tunneling Transport (with Eduardo Vaz): We have investigated sequential tunneling through a multilevel quantum dot confining multiple electrons in the regime where several channels are available for transport within the bias window. By analyzing solutions to the master equations of the reduced density matrix, we have derived general conditions on when the presence of a second transport channel in the bias window quenches transport through the quantum dot.

2) Hyperfine-Induced Decoherence (with Jean-Marc Samson): We approach the study of the electron spin decoherence due to the Fermi contact hyperfine interaction with the density matrix formalism of quantum relaxation. We consider an s-type electron in the ground state of a quantum dot interacting with a thermal distribution of nuclear spins. We directly compute the time dependence of the reduced density matrix by solving the system of integro-differential equations resulting from the Liouville equation at the Born (but not Markov) approximation. We show how the spin precession can, under certain circumstances, slow down and even reverse its rotation sense.

3) Quantum Computing (with Guido Burkard): We have proposed a universal quantum computing scheme in which the orthogonal qubit states are identical in their single-particle spin and charge properties. Each qubit is contained in a single quantum dot, and gate operations are induced all electrically by changes in the confinement potential. Within the computational space, these qubits are robust against environmental influences that couple to the system through single-particle channels. Due to the identical spin and charge properties of the qubit states, the lowest-order relaxation and decoherence rates $1/T_1$ and $1/T_2$, within the Born-Markov approximation, both vanish for a large class of environmental couplings.

The above projects all rely on similar computational frameworks, and I'll describe approaches which have worked for us, the problems we have encountered, how we overcame (some of) them, and what we're trying to do next.

Piezoelectric effect and spontaneous polarization in GaN/AlN quantum dots

B. Lassen¹, M. Willatzen¹, D. Baretin¹, R. V. N. Melnik² and L. C. Lew Yan Voon³

¹ The Mads Clausen Insitute, The University of Southern Denmark, Denmark

² Wilfrid Laurier University, Ontario, Canada

³ Department of Physics, Wright State University, Ohio, USA

October 1, 2007

It is well known that strain due to lattice mismatch in nanoscale semiconductor heterostructures gives important contributions to electronic properties, e.g., it has been shown [1] how to use strain to minimize the effective mass at the valence-band edge in quantum wells. The impact of the piezoelectric effect on the near-bandgap electronic structure and the effect of piezoelectricity and spontaneous polarization on the strain fields and the electric potential have been studied by several groups in the past decade [2, 3, 4, 5, 6, 7, 8, 9, 10]. One of the key questions has been whether it is reasonable to use a semi-coupled model where the strain due to lattice mismatch is calculated first without coupling to the electric field and then inserted into the equation for the electric displacement field. It turns out that the semi-coupled model is adequate for some materials (e.g. InGaN/GaN) but fails for other materials (e.g. GaN/AlN) [8]. Furthermore, results indicate that for a GaN/AlN heterostructure, the spontaneous polarization is just as important as the piezoelectric effect [3, 8].

In this work we study the influence of the piezoelectric effect and spontaneous polarization on the electronic structure of a GaN/AlN quantum dot. We employ the wurtzite 6-band $k \cdot p$ model for the upper valence band structure and the 1-band model for the lower conduction band structure [6]. We assume that the dot is cylindrically symmetric around the c -axis. Although wurtzite quantum dots are usually found with a hexagonal pyramidal structure we do not expect to find major differences between hexagonal and cylindrically symmetric structures. This has recently been asserted for wurtzite nanowires [11]. Due to the fact that the $k \cdot p$ model and the system of coupled equations for the strain and the electric fields are cylindrically symmetric around this axis [12, 13] the cylindrical geometry enables us to reduce the complete model to a two-dimensional problem.

References

- [1] E. P. O'Reilly and G.P. Witchlow. *Phys. Rev. B*, 34, 6030, 1986.
- [2] J. Wang, J. B. Jeon, Yu. M. Sirenko, and K. W. Kim. *IEEE Photonics Technology Letters*, 9, 728, 1997.
- [3] S. H. Park and S. L. Chuang, *Journal of Applied Physics*, 87, 353, 2000.
- [4] E. Pan. *Journal of Applied Physics*, 91, 3785, 2002.
- [5] B. Jogai, J. D. Albrecht, and E. Pan. *Journal of Applied Physics*, 94, 3984, 2003.

- [6] V. A. Fonoberov and A. A. Balandin. *Journal of Applied Physics*, 94, 7178, 2003.
- [7] U. M. E. Christmas, A. D. Andreev, and D. A. Faux. *Journal of Applied Physics*, 98, 073522, 2005.
- [8] M. Willatzen, B. Lassen, and L. C. Lew Yan Voon. *Journal of Applied Physics*, 100, 024302, 2006.
- [9] A. D. Andreev and E.P. O'Reilly. *Physica E*, 10, 553, 2001.
- [10] T. Saito and Y. Arakawa. *Physica E*, 15, 169, 2002.
- [11] B. Lassen, M. Willatzen, R. Melnik, and L. C. Lew Yan Voon. *Journal of Materials Research*, 21, 2927, 2006.
- [12] L. C. Lew Yan Voon, C. Galeriu, B. Lassen, M. Willatzen, and R. Melnik. *Applied Physics Letters*, 87, 041906, 2005.
- [13] D. Baretin *et al.*, Poster presented at Banff, Workshop 07w5057, *Physics-Based Mathematical Models of Low-Dimensional Semiconductor Nanostructures: Analysis and Computation*.

Nano Mechanics of Contact: Adhesion and Hysteresis

Adrian Lew

The phenomenon of hysteresis without plastic deformation as observed in nanoscale contact experiments is not well understood. Understanding the mechanics and hysteresis during contact at nanoscale is important for the quantitative mapping of Nanomechanical properties. Unfortunately existing continuum theories of contact mechanics do not capture the phenomenon of hysteresis during elastic contact.

Atomistic simulation studies reveal that the presence of short-ranged adhesive forces between the two bodies can be responsible for a hysteretic behavior that is different than the traditional pull-in-pull-out instability, and that presents features that are consistent with a number of experimental results with AFM. We constructed a simple model to explain this behavior, and interestingly, it reveals that the proposed mechanism would not be observed in a continuum limit, but only if the discrete nature of the atomistic lattice is accounted for. If such an effect is in fact present, it would therefore be a truly nanoscale phenomenon that only AFM measurements could resolve.

Multiscale Nonequilibrium Molecular Dynamics and Direct Simulation of Phonon Scatterings

BY SHAOFAN LI

*Department of Civil and Environmental Engineering,
University of California, Berkeley, CA94720, USA*

Abstract

Recently, we have developed a novel multiscale nonequilibrium dynamics (MS-NEMD), which is capable of simulating coupled thermal-mechanical coupling at small scales, such as nanoscale heat conduction and phonon scatterings by defects, e.g. dislocations and cracks.

Because the traditional NEMD is in fact a local micro-canonical ensemble simulation, it lacks a solid statistical physics foundation for ensemble thermal-mechanical simulations at temperatures higher than Debye temperature.

The proposed MS-NEMD is a multiscale paradigm for steady-state non-equilibrium thermodynamic systems. It consists of coupled dynamics at two-scales: (1) a nonequilibrium coarse grained thermodynamics that provide a deterministic description for “the mean field” or the drift field, and (2) a fine scale molecular dynamics with atomistic resolution. A distributed Nosé-Hoover thermostat network couples the two dynamics. The construction of distributed Nose-Hoover thermostat network, or the non-uniform distributed thermo-reservoirs, is based on the local equilibrium assumption, and it is a generalization of classical concept of thermal reservoir. The distributed thermal reservoir is a discrete network, whose temperature at each finite element node is fixed during a macro time step. So it can provide correct random forces and regulates thermal fluctuations in the fine scale. We have shown that under the proposed MS-NEMD framework, in each finite element cell ensemble the distribution function obeys a drifted Maxwell-Boltzmann distribution, i.e. it is locally canonical.

By bridging these two dynamics, we are able to simulate phonon scatterings and related nanoscale heat transfer at small scale via direct simulation. To validate the proposed algorithm, we have used MS-NEMD to simulate the thermal activation of dislocation or shock waves propagations under nonequilibrium states, and we have compared the results with equilibrium ensemble MD and traditional NEMD. The numerical results have shown the potential of the MS-NEMD algorithm.

Atomistic Treatment of Electronic Transport: The Effect of Bandstructure

Neophytos Neophytou and Gerhard Klimeck

Electrical and Computer Engineering, Network for Computational Nanotechnology,
Purdue University, West Lafayette, IN, 47907, USA

e-mail: neophyto@purdue.edu

As device sizes shrink to the nanoscale, CMOS development investigates alternative structures and devices. Existing CMOS devices will evolve to 3D non-planar devices at nanometer sizes. They will operate under strong confinement and strain, regimes where atomistic effects are important. Under these conditions, effects that were absent in the previous technology nodes, appear, and in several cases dominate the performance of electronic devices.

Some of these effects are non-parabolicities and anisotropies in the electronic structure, strong coupling of bands, degenerate valley splittings due to enhanced quantum interactions, strain, material and potential variations on the nanoscale. Traditional electronic transport simulation methods usually deal with effective mass approximations, often with a simple treatment of non-parabolicity effects. Under strong quantization at nanometer scales, however, these methods will break down. Simple analytic effective mass approximations are not able any more to describe the electronic structure of materials, and more sophisticated models need to be utilized that will treat the channels all the way down to atomistic sizes. Such a model is the $sp^3d^5s^*$ -SO nearest-neighbor tight-binding model (or LCAO for Local Combination of Atomic Orbitals) [1].

In this model, each atom in the channel of the transistor is modeled by a basis set of 10 orbitals (this becomes 20 if Spin-Orbit is included). It is demonstrated to correctly reproduce the bulk bandstructure of silicon, germanium and III-V semiconductor materials, and be able to predict quantities such as the bandgap of highly quantized nanowire devices. The effects that appear in quantized systems mentioned above are also accounted for in this model, once the fitting parameters in the model are calibrated. A genetic algorithm is utilized for this purpose. The electronic structures of these materials look very different and examples will be presented in the poster. Strong variation in various quantities such as the effective masses and valley splittings that appear for example in small nanowires will also be addressed.

Other than material dependent, the electronic structure is geometry dependent and also a sensitive function of the potential variation and charge filling of the lattice [2]. The interactions between the different valleys and the position of the quantized levels, especially under potential variations in the lattice do not follow simple “particle in a box” rules, but behave in a non-trivial way that needs modeling with atomistic representation in order to be captured.

In summary, atomistic treatment is essential in ultra scaled electronic devices, and tight-binding models such as the $sp^3d^5s^*$ -SO model is an effective one to capture a lot of the important bandstructure effects that dominate transport. Community tools for efficient and rigorous computation of such effects are of great help for the community. The nanoHUB.org serves as an engine that hosts nanotechnology community tools such as bandstructure calculation tools [3].

Acknowledgement

This work was supported by the Semiconductor Research Corporation (SRC) and Microelectronics Advanced Research Focus Center on Materials, Structures and Devices (MARCO). nanoHUB.org computational resources were used in this work.

References

- [1] G. Klimeck, F. Oyafuso, T. B. Boykin, R. C. Bowen, and P. von Allmen, Computer Modeling in Engineering and Science (CMES) Volume 3, No. 5 pp 601-642 (2002).
- [2] N. Neophytou, A. Paul, M.S. Lundstrom and G. Klimeck, SISPAD, 2007
- [3] Bandstructure lab on nanoHUB.org (<https://www.nanohub.org/tools/bandstrlab/>)

A Level Set Simulation of Directed Self-Assembly during Epitaxial Growth

X.B. Niu,¹ Y-J Lee,² R.E. Caflisch,^{1,2} and C. Ratsch^{2,3}

¹*Department of Materials Sciences and Engineering, University of California, Los Angeles, Los Angeles, California 90095, USA*

²*Department of Mathematics, University of California, Los Angeles, Los Angeles, California 90095, USA*

³*Institute for Pure and Applied Mathematics, University of California, Los Angeles, Los Angeles, California 90095, USA*

We study the effect of a spatially varying potential energy surface on the self-organization of nanoscale patterns during epitaxial growth. The computational approach is based on the level set method. Our results have implication for guided self-assembly of nano patterns, which is a promising new technique for many technological applications. Both, kinetic as well as thermodynamic effects can lead to ordering, and we discuss the competition between these two effects.

Theory of the band structure of extreme semiconductor alloys

E.P. O'Reilly and A. Lindsay

Tyndall National Institute, Lee Maltings, Cork, Ireland

There has been considerable interest in extreme semiconductor alloys such as $\text{Ga(In)}\text{N}_x\text{As}_{1-x}$ and $\text{GaN}_x\text{P}_{1-x}$. The band-anticrossing (BAC) model describes the rapid reduction of energy gap with composition in $\text{GaInN}_x\text{As}_{1-x}$ in terms of an anti-crossing interaction between the host matrix conduction band edge and a single band of N resonant defect states, with the general increase of electron effective mass also explained through this interaction. Although the BAC model explains qualitatively the behaviour of dilute nitride alloys, it fails to provide an accurate quantitative description of many experimental results, including the observed variation with N composition x of the electron effective mass and gyromagnetic ratio, and the electron mobility in $\text{GaN}_x\text{As}_{1-x}$. It also cannot account for the observed evolution of the lowest conduction states in the indirect gap alloy $\text{GaN}_x\text{P}_{1-x}$.

Detailed theoretical and experimental studies show a wide range of N states above and close to the conduction band edge in $\text{GaN}_x\text{As}_{1-x}$, due to the formation of N-N pairs, where a group III atom has two neighbouring N atoms, and due to the formation of other, larger, N clusters. We show that a modified BAC model, which treats explicitly the interactions between the host conduction band edge and this distribution of N states explains quantitatively both the observed non-monotonic variation of effective mass and gyromagnetic ratio with composition (see Fig. 1), and also the generally low values of electron mobility observed in GaNAs samples.

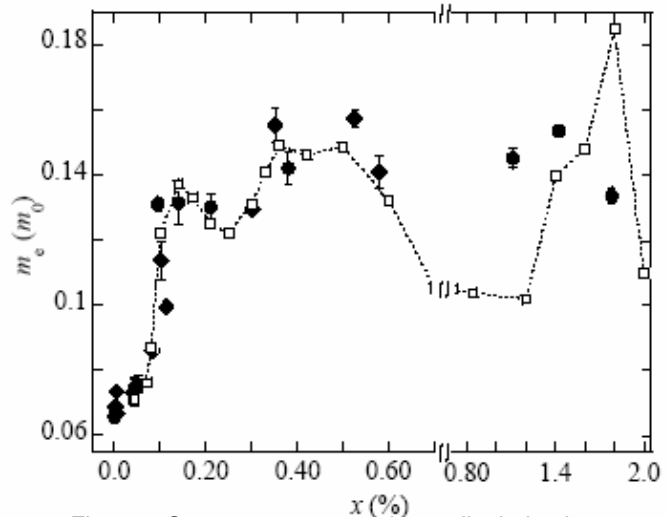


Figure 1 Open squares: experimentally derived variation of electron effective mass with composition x in $\text{GaN}_x\text{As}_{1-x}$. Solid circles: calculated values including distribution of N states (from [1])

Turning to $\text{GaN}_x\text{P}_{1-x}$, the BAC model provides qualitative understanding but fails to describe the evolution of N-related states in this case. Band structure calculations show that a two-level BAC model describes the lowest states in ordered GaNP supercells. Photocurrent and photoreflectance measurements confirm a BAC-related blue shift of the GaP-like lowest direct band gap in disordered GaNP, but calculations, electromodulated absorption and pressure studies show that the wide energy distribution of the lower-lying N-related states leads to the anti-crossing interaction being distributed over many N levels in disordered GaNP.

Finally, we consider the wider application of BAC models, both to other III-(N,V) alloys and also to (B,III)-V alloys. The conduction band structure of $\text{B}_x\text{Ga}_{1-x}\text{As}$ has a near-linear blue-shift of the energy gap, which can be described using the virtual crystal approximation, but a dramatic increase in the band edge effective mass m_e at low B composition, similar to that observed in $\text{GaN}_x\text{As}_{1-x}$. We show that isolated B

atoms have little effect either on the band gap or lowest conduction band dispersion in $B_xGa_{1-x}As$. By contrast, B pairs and clusters introduce defect levels close to the band edge which, through a weak BAC interaction, significantly reduce the band dispersion in and around the Γ -point, thus accounting for the strong increase in m_e and reduction in mobility observed in these alloys.

We conclude that key aspects of the band structure of the extreme III-(V,N) and (III,B)-V semiconductor alloys can be well described using simple BAC-type models, but that the detailed distribution of N or B defect-like states needs to be considered for a quantitative analysis of the band structure and its consequences. We argue that the unique electronic structure of dilute nitride and boride alloys enables wide possibilities that are only now starting to be considered. These include a new class of infrared avalanche photodiode with superior performance and greater ease of fabrication, compatible with GaAs-based technology, as well as AlGaInNAsP alloys lattice-matched to Si for efficient high-speed infra-red optical sources compatible with silicon technology. We argue that our detailed models provide the best approach to analyse and address the many challenges to achieve these and related goals.

[1] F. Masia, G. Pettinari, A. Polimeni, M. Felici, A. Miriametro, M. Capizzi, A. Lindsay, S.B. Healy, E.P. O'Reilly, A. Cristofoli, G. Bais, M. Piccin, S. Rubini, F. Martelli, and A. Franciosi, P. J. Klar, K. Volz, and W. Stolz, *Phys. Rev. B* **73**, 073201 (2006)

MULTISCALE MODELS TO CAPTURE SURFACE STRESS EFFECTS ON METALLIC AND SEMICONDUCTING NANOWIRES

Harold S. Park^a, Patrick A. Klein^b and Geng Yun^a

^aDepartment of Mechanical Engineering
University of Colorado at Boulder
Boulder, CO 80309
harold.park@colorado.edu

^bFranklin Templeton Investments
San Mateo, CA 94403

We present a novel hierarchical multiscale model, the surface Cauchy-Born (SCB) model, which was recently developed to capture surface stress effects on the mechanical behavior and properties of nanowires. We will show that the SCB model is unique as it enables the solution of 3D nanomechanical boundary value problems for displacements, stresses and strains in nanomaterials using standard nonlinear finite element (FE) techniques while accounting for surface stress effects on the mechanical response. The theory will be presented for both metallic and semiconducting nanowires, while verification of the method will focus on capturing the minimum energy configurations of both metallic and semiconducting nanowires due to surface stresses as compared to benchmark fully atomistic calculations. Numerical examples will focus on applying the SCB model for FCC metals to: (1) Calculations of the resonant frequencies, and thus the elastic properties of metallic nanowires, and 1D numerical examples involving: (2) Nanoscale resonant mass sensing, and (3) Modeling surface stress effects on the thermoelastic properties of nanostructures.

References

- [1] H.S. Park, P.A. Klein and G.J. Wagner. “A Surface Cauchy-Born Model for Nanoscale Materials”, *International Journal for Numerical Methods in Engineering* 2006; 68:1072-1095.
- [2] H.S. Park and P.A. Klein. “Surface Cauchy-Born Analysis of Surface Stress Effects on Metallic Nanostructures,” *Physical Review B* 2007; 85:085408.
- [3] H.S. Park and P.A. Klein. “Surface Stress Effects on the Resonant Properties of Fixed/Fixed Metal Nanowires”, submitted to *Physical Review B* 2007.
- [4] G. Yun and H.S. Park. “Surface Cauchy-Born Modeling of Nanoscale Resonant Mass Sensing”, submitted to *Computer Methods in Applied Mechanics in Engineering* 2007; Special issue on Computational Study of Nanostructures.
- [5] G. Yun and H.S. Park. “A Multiscale, Finite Deformation Formulation for Surface Stress Effects on the Coupled Thermomechanical Behavior of Nanomaterials”, submitted to *Computer Methods in Applied Mechanics and Engineering* 2007; Special issue on Computational Study of Nanostructures.
- [6] H.S. Park and P.A. Klein. “A Surface Cauchy-Born Model for Silicon Nanostructures”, submitted to *Computer Methods in Applied Mechanics and Engineering* 2007; Special issue on Computational Study of Nanostructures.

From atomic to $k\cdot p$ calculations applied to semiconductor heterostructures

L. Pedesseau^a, C. Cornet^a, F. Doré^a and J. Even^a
A. Schliwa^b and D. Bimberg^b

^a*FOTON-INSA Laboratory, UMR 6058 au CNRS, INSA de Rennes, 20 avenue des Buttes de Coëmes, CS 14315, 35043 RENNES Cedex, FRANCE*

^b*Institut für Festkörperphysik, Technische Universität Berlin, Hardenbergstrasse 36, 10623 Berlin, Germany*

Abstract. We present a brief overview of the main results obtained in our group for the simulation of electronic and optical properties of semiconductor heterostructures. A short introduction is given on InAs quantum dots, grown on InP, GaAs and GaP substrates. A study of the highly strained InAs/GaP interface is performed with a first principle modeling using ABINIT packages. Band lineups are calculated, and compared to those found by Chuang et al. [1] A complete 8*8 band $k\cdot p$ approach is then used to show the properties of InAs/InP quantum dots, with different substrate orientation. A semianalytical modeling is also presented, including an axial approximation of the 8*8 band $k\cdot p$ calculations. Linear and non-linear contributions to piezoelectricity are discussed. Finally, it is shown that the $k\cdot p$ calculations can be used in the reciprocal space, in order to get a simulation of perfectly ordered array of quantum dots.

Introduction to InAs quantum dots

Recently there have been considerable research developments in the field of nano-structured semiconductor materials. In particular, quantum dots (QDs) may improve the properties of high performance optoelectronic devices as compared to that achieved with semiconductor quantum wells.[2] One of the biggest challenges for QD-optical-devices however is to reach specific wavelength with respect to targeted applications. In this respect, various materials associations are used. In our group, we devoted our researches to the study of InAs quantum dots. Using InAs/InP or InAs/GaAs QDs allows reaching respectively the 1.55 μm (0.8 eV) and 1.3 μm (0.95 eV) telecommunication wavelengths. In a more original approach, InAs/GaP QDs could be used to emit under the transparency region of the Silicon (>1.1 μm) for optical interconnection compatible with MOSFET technology.

In this regard, calculations of electronic and optical properties of quantum dots are a key step in the development of QDs-based applications. The simulation of QDs properties is most of the time performed using either atomistic models, such as the empirical pseudopotential theory,[3,4] or continuum models, such as the eight-band $k\cdot p$ theory. [5,6]

Atomic calculations: band lineups by abinitio calculations

Our aim is to compare the valence band line-up of InAs/GaP from existing calculations by Chuang [1] with *Ab initio* calculations. We perform our calculations using the density functional theory. We consider the crystal bulk of InAs and GaP with the local density approximation

(LDA) as pseudopotential. We do not include spin-orbit (SO) splitting in both calculations. A correction via the GW approximation is made on each valence band. Band lineups for strained InAs on GaP are thus determined. A good agreement is found between the Chuang and *Ab initio* calculations. Evolution of the InAs gap energies for different biaxial deformations is also studied.

Complete 8*8 k·p approach

A complete study of InAs/InP quantum dots by 8*8 band k·p calculations is then presented.[6] Impact of substrate orientation and truncation height on optical properties is examined carefully, with respect to experimental datas. A good agreement is found, and the importance of strain and piezoelectric field is pointed out.

Semi-analytical resolution by axial approximation

A complete semi-analytical model is then proposed for the simulation of the electronic, mechanical and piezoelectric properties of narrow gap strained semiconductor quantum nanostructures. A transverse isotropic approximation for the strain and a new axial approximation for the strained 8x8 Hamiltonian are proposed. It is applied extensively to the case of InAs/InP quantum dots (QD). Symmetry analysis shows that it does exist a non-vanishing splitting on the electron P states, due to the coupling with valence band. This splitting is found to be smaller in InAs/GaAs QD than in InAs/InP QD. Analytic expressions for the first and second order piezoelectric polarizations are proposed.[7]

k·p approach in the reciprocal space

Finally, we present an original approach to simulate the properties of laterally organized array of quantum dots.[8] Using the Fourier-transformed Schrödinger equation developed on a mixed basis, we describe the wetting layer-assisted inter-QDs lateral (WLaiQD) coupling by studying the influence of wetting layer (WL) states on QDs states and vice-versa. The results show that WL and QDs have to be considered as a unique system, in strong coupling conditions. The increase of QDs density on the WL leads to enhanced splitting and minibands effects on QDs states. It induces a fragmentation of WL density of states interpreted as a 0D-like confinement of WL states.

References

- [1] S.-L. Chuang, "Physics of optoelectronic devices." Wiley Series in pure and Applied Optics, Joseph W. Goodman, Series Editor, 1995.
- [2] M. Grundmann, D. Bimberg and N.N. Ledentsov, *Quantum Dot Heterostructures* (Chichester: Wiley, 1998).
- [3] G. Bester and A. Zunger, *Phys. Rev. B* **71**, 045318-12 (2005).
- [4] G. Bester, X. Wu, D. Vanderbilt and A. Zunger, *Phys. Rev. Lett.* **96**, 187602-4 (2006).
- [5] O. Stier, M. Grundmann and D. Bimberg, *Phys. Rev. B* **59**, 5688-5701 (1999).
- [6] C. Cornet, A. Schliwa, J. Even, F. Dore, C. Celebi, A. Letoublon, E. Mace, C. Paranthoen, A. Simon, P. M. Koenraad, N. Bertru, D. Bimberg and S. Loualiche, *Phys. Rev. B* **74**, 035312 (2006).
- [7] J. Even, F. Doré, C. Cornet, L. Pédesseau, A. Schliwa and D. Bimberg, *Appl. Phys. Lett.* **91**, 122112 (2007).
- [8] C. Cornet, C. Platz, P. Caroff, J. Even, C. Labbé, H. Folliot, A. Le Corre and S. Loualiche, *Phys. Rev. B* **72**, 035342 (2005)

Nonlinear Strain, Polarization and Size Effects in Quantum Confinement of Semiconductor Heterojunction

D. Roy Mahapatra^{a,1} and R. Melnik^b

^aDepartment of Aerospace Engineering, Indian Institute of Science,
Bangalore 560012, India

^bM²NeT Lab, Wilfrid Laurier University, Waterloo, ON N2L3C5, Canada

Abstract

Size effect is an important factor in the design of quantum dots and quantum wires. During the growth of crystals in the shape of a target heterostructure, pile-up of residual stress, crystal plasticity, phase transformation induced inhomogeneity and lattice defects are common. Although wide-bandgap materials are ideal for high mobility heterojunction and for larger quantum confinement, however the inhomogeneous material properties often give rise to adverse effects on the quantum confinement and tunneling characteristics [1]-[4]. In this context, we develop a self-consistent modeling framework, wherein various coupling issues within the framework of nonlinear crystal piezoelectricity and $k \cdot p$ theory for analyzing quantum confinement are considered. A variational formulation results in a Poisson-Navier-Schrodinger system which is solved by finite element method. With this computational technique, we then analyze (1) the effects of nonlinear strains (2) the effects of piezoelectricity and spontaneous polarization and (3) the effect of diffused interfaces on the size and intensity of quantum confinement. Here we consider $\text{Al}_x\text{Ga}_{(1-x)}\text{N}/\text{GaN}$ multilayer system. Figure 1 shows the variations in the strain field due to volume fraction of GaN in the AlGaN barrier layer, which in turn affects the bandgap. These results are based on smooth distribution of lattice constants $a(\bar{z})$ with $\bar{z} \in [z_0, z_0 + l]$ as the local coordinate. Here l is the width of the diffused $\text{Al}_x\text{Ga}_{(1-x)}\text{N}/\text{GaN}$ interface. By denoting the aluminum fraction as $p = 1 - x$, the following distribution has been incorporated in the model;

$$a(\bar{z}) = a_{\text{GaN}} + p(a_{\text{GaN}} - a_{\text{AlN}}) \left[3 \left(\frac{\bar{z}}{l} \right)^2 - 2 \left(\frac{\bar{z}}{l} \right)^3 \right], \quad (1)$$

¹Corresponding author e-mail: droymahapatra

which is obtained by matching the lattice constants on the two sides of the diffused interface using a cubic polynomial fit. Detailed numerical simulation will be discussed.

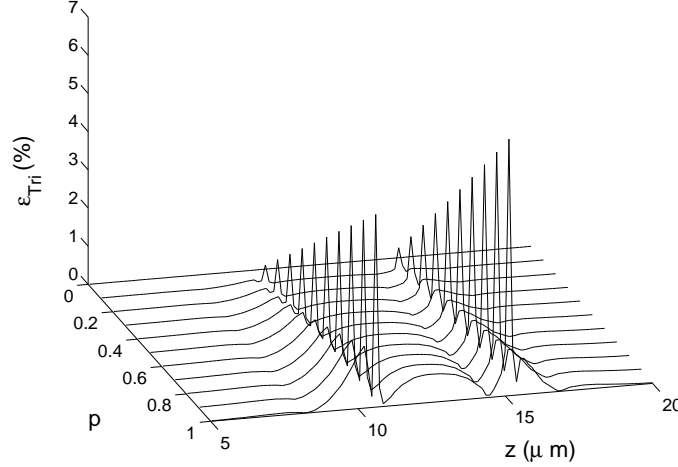


Figure 1: (a) Variation in the tri-axial strain as function of volume fraction $p = 1 - x$ in the diffused interfaces surrounding the barrier layer of $\text{Al}_x\text{Ga}_{(1-x)}\text{N}$.

References

- [1] Coupled effects in quantum dot nanostructures with nonlinear strain and bridging modelling scales, R.V.N. Melnik and Roy Mahapatra, *Computers and Structures*, 85, 698-711, 2007.
- [2] Effects of electromechanical coupling on the strain in AlGa_N/Ga_N heterojunction field effect transistors, B. Jogai, J.D. Albrecht, E. Pan, *J. Appl. Phys.* 94(6), 3984-3989, 2003.
- [3] Simulation on the effect of non-uniform strain from the passivation layer on AlGa_N/Ga_N HEMT, M.A. Mastro, J.R. LaRoche, N.D. Bassim, C.R. Eddy Jr., *Microelectronic Journal*, 36, 705-711, 2005.
- [4] Non-linear strain theory for low-dimensional semiconductor structures, B. Lassen, R. Melnik, M. Willatzen, L.C. Lew Yan Voon, *Nonlinear Analysis*, 63, 1607-1617, 2005.

Constructing mathematical models for quantum devices through experimental system identification

Sonia G Schirmer,^{1,*} Daniel Oi,² Simon J. Devitt,³ and Jared Cole⁴

¹*Dept of Applied Maths & Theoretical Physics, University of Cambridge, Wilberforce Rd, Cambridge, CB3 0WA, UK*

²*Dept of Physics, Strathclyde University, Glasgow G1 1XQ, UK*

³*National Institute of Informatics, 2-1-2 Hitotsubashi, Chiyoda-ku, Tokyo 101-8430, Japan*

⁴*School of Physics, University of Melbourne, Melbourne, Victoria 3010, Australia*

We consider the problem of intrinsic control system identification for quantum devices. We will outline a simple general strategy for full Hamiltonian identification of a controlled two-level system, and then consider identification of decoherence processes, and the generalization of the protocols to higher dimensional systems.

Advances in nano-fabrication increasingly make it possible to create nano-scale devices which exhibit non-classical or quantum mechanical behaviour. Such 'quantum' devices are of great interest as they may pave the way for a new generation of 'quantum technology' with various applications from quantum metrology to quantum information processing. However, in order to create quantum devices that perform useful functions, we must be able to understand their behaviour, and have means to controllably manipulate it to suit a certain purpose. Analysis of system behaviour and the design of effective control strategies is almost impossible without the availability of sufficiently accurate mathematical models of the device. While these models should capture the essential features of the device, they must be computationally tractable, and preferably as simple as possible.

The problem is further complicated by the variability of manufactured systems such as artificial quantum dot 'atoms' and 'molecules' as a result of the manufacturing process. The complexity of these structures, involving many atoms in the solid state, and their intrinsic variability, make it often difficult to derive accurate models for them from first principle calculations. An alternative approach is to try to experimentally characterize the intrinsic dynamics of the system including its interaction with the control and measurement apparatus. An interesting question in this context is under which conditions, we can build a phenomenological model of the system based on observations of its dynamics, which suffices to make accurate predictions about its behaviour, and if so, how to best go about it. Although, there are some tools available to do this, such as various forms of spectroscopy and tomography, in most situations, it is non-trivial to extract a complete model of the system including its interaction with the controller.

For instance, consider a double-dot system controlled by several gate electrodes with a single electron transistor as a readout device as shown in Fig. 1. Assume the state of the system is described by a density operator $\rho(t)$ which evolves according to the quantum Liouville

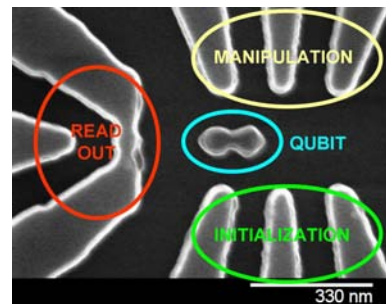


FIG. 1: Simple charge 'qubit' device: Si double-dot controlled by DC-gate electrodes with SET for charge readout (Hitachi Cambridge Labs).

equation

$$\frac{d}{dt}\rho(t) = -\frac{i}{\hbar}[H, \rho(t)] + L_D[\rho(t)], \quad (1)$$

where H is the (effective) Hamiltonian and L_D a superoperator that accounts for dissipative effects due environmental influences. A mathematical model of the system in this case requires knowledge of the Hamiltonian H and the dissipator L_D , both of which may depend on the voltages V_m applied to various control electrodes, i.e., $H = H(\mathbf{V})$ and $L_D[\rho(t)] = L_D[\mathbf{V}][\rho(t)]$, where $\mathbf{V} = (V_m)_{m=1}^M$. Neither standard spectroscopic techniques nor process tomography can easily provide this information. In fact, without additional resources we cannot perform tomography at all as we only have single readout channel and no a priori knowledge of the Hamiltonian.

Nonetheless, it is possible to completely characterize the control dependent Hamiltonian $H(\mathbf{V})$ and certain (common) decoherence processes L_D by systematically mapping out coherent oscillations of the system in a stroboscopic fashion (see Fig. 2) given a single fixed readout channel. For a system that can be modelled as a two-level system (qubit) the process of Hamiltonian identification is quite straightforward [1], and using tools from Fourier analysis, for instance, we can easily derive estimates for the uncertainty of certain parameters and the experimental overhead required [2], even in the presence of decoherence [3].

*Electronic address: sgs29@cam.ac.uk

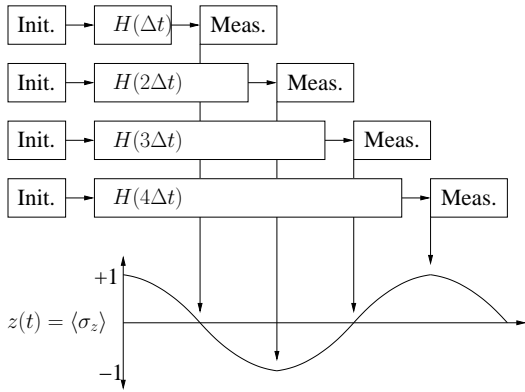


FIG. 2: Stroboscopic mapping of coherent oscillations induced by controls with projective measurement. After initialization through measurement, the system is allowed to evolve for fixed times under the influence of the controls before a second measurement is taken. The experiments are repeated to determine the expectation value of the observable at each time.

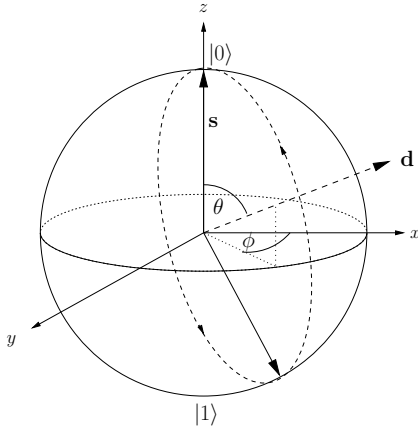


FIG. 3: Evolution of a two-level system under a fixed Hamiltonian is equivalent to a rotation around a fixed axis $\mathbf{d}(\theta, \phi)$ in R^3 with frequency ω .

We will briefly describe a simple protocol for full Hamiltonian and dissipator identification for two-level systems, and then consider various extensions to higher dimensional systems such as D -level systems (qudits) [4] or systems of interacting qubits [5]. One problem for

higher dimensional systems is that many more parameters need to be identified – a fixed Hamiltonian for a two-level system is fully characterized by three parameters, two angles (θ, ϕ) determining the orientation of the rotation axis and a rotation frequency ω (see Fig. 3) while a generic Hamiltonian for a d -level system (for fixed control settings) is specified by $d^2 - 1$ parameters. The number of parameters required to determine L_D increases even faster, even when the decoherence processes are restricted. This means identification protocols become more complicated and more experiments are required.

In addition, more independent control electrodes (or similar) may be available to manipulate the dynamics, increasing the number of possible control settings for which the dynamics needs to be characterized, and complications such as cross-talk between control electrodes may arise, requiring additional experiments to characterize. Furthermore, while coherent oscillations of a two-level system are always 'monochromatic', the oscillations for higher dimensional systems will be 'polychromatic', i.e., containing multiple frequency components. Although such problems can be addressed using, e.g., harmonic decomposition techniques, more measurement repetitions per time point will be required to resolve the resulting multi-frequency oscillations.

In certain special cases, identification protocols may be simplified. For example, in the special case of two interacting qubits, where we have full local control, which has been characterized separately, and the interaction Hamiltonian is known to be fully non-local, as might be the case, e.g., for two individually controllable spins with fixed (non-controllable) Ising or Heisenberg coupling, an alternative strategy to determine the interaction Hamiltonian is mapping of the concurrence of the system [6].

The characterization protocols above assume that the dimension of the system to be modelled is known. However, in many cases the system we are interested in is likely to be embedded in a larger system, which may result in 'leakage' of population out of the subspace, especially when control fields are applied. It is therefore highly desirable to independently estimate subspace confinement, and protocols for doing this, should do not require the ability to measure or control the super-system. In general this is a very difficult task but we will discuss a simple protocol for a single 'qubit' [7].

-
- [1] S. G. Schirmer, A. Kolli, and D. K. L. Oi, Phys. Rev. A **69**, 050603(R) (2004).
 [2] J. H. Cole, S. G. Schirmer, A. D. Greentree, C. J. Wellard, D. K. L. Oi, and L. C. L. Hollenberg, Phys. Rev. A **71**, 062312 (2005).
 [3] J. H. Cole, A. D. Greentree, D. K. L. Oi, S. G. Schirmer, C. J. Wellard, and L. C. L. Hollenberg, Phys. Rev. A **73**, 062333 (2006).
 [4] S. Schirmer *et al*, Experimental characterization of con-

- trolled d -level systems (in preparation).
 [5] S. G. Schirmer *et al*, Experimental characterization of controlled two-qubit systems (in preparation).
 [6] S. J. Devitt, J. H. Cole, and L. C. L. Hollenberg, Phys. Rev. A **73**, 052317 (2006).
 [7] S. J. Devitt, S. G. Schirmer, D. K. L. Oi, J. H. Cole, L. C. L. Hollenberg, Subspace confinement: How good is your qubit? New J. Phys. (to appear)

Dipole nanolaser

I.E.Protsenko¹, A.V.Uskov¹, and E. P. O'Reilly²

¹*Lebedev Physical Institute, Leninsky prospect 53, Moscow, Russia*
²*Tyndall National Institute, Lee Maltings, Prospect Row, Cork, Ireland*

Upon definite conditions (“above threshold”) in the system “metal nano-particle” plus “two-level system” (say, Quantum Dot) coherent optical polarization is generated (“lased”). In turn, this coherently oscillating polarization can, in proper conditions, emit dipole radiation.

The Fastest 3D NEGF Solver: The Contact Block Reduction Method and its Application to Real Devices Modeling of the Presence and of the Future

D. Vasileska, D. Mamaluy and H. Khan
Arizona State University, Tempe, AZ 85287-5706, USA

Nowadays, semiconductor nanostructures are commonly employed in electronic and optoelectronic devices. Superlattices and quantum-wells have already penetrated the marketplace. Electronic devices such as the high electron mobility transistor have already shown outstanding performances pushing the cut-off frequencies up to several hundred of GHz [i,ii]. The successful realization of semiconductor nanostructures such as quantum dots [iii,iv], electron waveguide structures [v,vi,vii], molecules [viii,ix,x,xi] and, importantly, *nanoscale* metal-oxide semiconductor field-effect transistors [xii,xiii] calls for reliable and accurate theoretical tools to predict their charge carrier transport. Quantum effects play a dominant role in many of these small size structures so that the applicability of the standard well-developed engineering tools based on a semi-classical transport description is very limited or even impossible.

There are a number of methods developed by solid state theorists over the last several decades to address the issue of quantum transport. Among the most commonly used in nanostructure calculations schemes are the Wigner-function approach [xiv], the Pauli master equation [xv], and the non-equilibrium Green's functions (NEGF) [xvi,xvii,xviii]. The growing popularity of the latest (sometimes referred to as the Keldysh or the Kadanoff–Baym) formalism is conditioned by its sound conceptual basis for the development of the new class of quantum transport simulators [xix]. Among its doubtless advantages are the clear physical conceptions, rigorous definitions, well-developed mathematical apparatus and flexibility of the algorithmization.

Developed over 40 years ago, the NEGF formalism only recently became numerically viable for modeling semiconductor devices. Even now, however, the *direct* application of the NEGF is not an option for the quantum transport problem in three-dimensional or even sufficiently “large” two-dimensional structures. Thus, the key to the successful application of the NEGF formalism to the quantum transport problem in semiconductor nanostructures is the numerical efficiency. The goal of this presentation is to present a NEGF method we have developed few years back that is numerically efficient and ready for engineering applications in 2D and 3D objects on the one hand, and rigorously quantum-mechanical on the other hand. We also present some very important results from the FinFET analysis, such as optimization of the device structure, process variation etc.

-
- i R. Lee Ross, Stefan P. Svensson, Paolo Lugli (eds.) *Pseudomorphic Hemt Technology and Applications*, NATO Asi Series.
 - ii Series E. Applied Sciences Vol 309 (1996).
 - iii D. K. Ferry, R. Akis, and J. P. Bird, *Superlattices and Microstructures* 23, 611 (1998).
 - iv W. Z. Shangguan, T. C. Au Yeung, Y. B. Yu, and C. H. Kam, *Phys. Rev. B* 63, 235323 (2001).
 - v H. Frohne, M. McLennan, S. Datta, *J. Appl. Phys.* 66, 2699 (1989).
 - vi P. A. Knipp and T. L. Reinecke, *Phys. Rev. B* 54, 1880 (1996).
 - vii S. Rotter, J.-Z. Tang, L. Wirtz, J. Trost, and J. Burgdörfer, *Phys. Rev. B* 62, 1950 (2000).
 - viii C. Berger, Y. Yi, Z. L. Wang, W. A. de Heer, *Appl. Phys. A* 74, 363 (2002).
 - ix M. B. Nardelli, J.-L. Fattebert, and J. Bernholc, *Phys. Rev. B* 64, 245423 (2001).
 - x C. Roland, V. Meunier, B. Larade, and H. Guo, *Phys. Rev. B* 66, 035332 (2002).
 - xi J. L. Mozos, P. Ordejon, M. Brandbyge, J. Taylor, and K. Stokbro, *Nanotechnology* 13, 346 (2002).
 - xii Z. Ren, R. Venugopal, S. Datta et. al., *IEDM* 715 (2000).
 - xiii W. Chen, L. F. Register, and S. K. Banerjee, *IEEE Trans. El. Dev.* 49, 652 (2002).
 - xiv P. Brodono, M. Pascoli, R. Brunetti, A. Bertoni, and C. Jacoboni, *Phys. Rev. B* 59, 3060 (1998).
 - xv M. V. Fischetti, *Phys. Rev. B* 59, 4901 (1998).
 - xvi R. Lake, G. Klimeck, R. C. Bowen, and D. Jovanovic, *J. Appl. Phys.* 81, 7845 (1997).
 - xvii A. Haque, A. N. Khondker, *J. Appl. Phys.* 87, 2553 (2000).
 - xviii D. Guan and U. Ravaioli, R.W. Giannetta, M. Hannan and I. Adesida, *Phys. Rev. B* 67, 205328 (2003).
 - xix Supriyo Datta, *Superlattices and Microstructures* 28, 253 (2000).

Atomistic Simulation of Nanosize Electronic Devices

Lin-Wang Wang

Lawrence Berkeley National Laboratory

When the size of an electronic device (e.g., metal-oxide semiconductor field effect transistor, MOSFET) shrinks to nanometers, the quantum mechanical effects become important. I will present a method which uses atomistic pseudopotentials to calculate the electronic structures and electrical properties (I-V curve, gate threshold voltage, gate capacitance) of the million atom devices. We use linear combination of bulk band (LCBB) method to solve the electron eigenstates of the system, and special formalism to occupy the eigenstates in an nonequilibrium system. Charge selfconsistent calculations are carried out in the simulations. I will discuss the quantum mechanical effects and single dopant fluctuations in such devices.

Computational Needs of Non-Conventional Semiconductor Nanostructures

Yong Zhang (yong_zhang@nrel.gov)
Materials and Computational Science Center
National Renewable Energy Laboratory (NREL), USA

Two classes of novel semiconductors are used to illustrate the computational challenges for modeling the physical properties of non-conventional semiconductor nanostructures. The first class is inorganic-organic hybrid semiconductors involving II-VI semiconductors and small organic molecules. The second class is core-shell semiconductor nanowires whose components have type II energy alignments and a relatively large lattice mismatch.

The hybrid structures are composed of nano- or subnano- scale slabs or chains of the inorganic component interconnected or coordinated by small organic molecules.¹ They are three-dimensional ordered structures. Although for the majority of them not much is known beyond the crystal structure, for a few of them selected physical properties have been investigated both experimentally and theoretically.¹⁻⁴ They have been shown to exhibit a number of unusual properties, for instance, a large bandgap blue shift (up to 2 eV), a strong enhanced exciton binding energy and band edge excitonic absorption (reaching 10^6 cm^{-1}), with respect to the inorganic component; and zero-thermal expansion. These unusual properties in turn offer various potential applications in areas like solid-state lighting, solar cells, UV detectors, transparent conducting materials.

Figure 1 shows the crystal structure of a prototype hybrid semiconductor, β -ZnTe(en)_{0.5}. This particular structure has a 32 atom unit cell, one of the smallest among the hybrid structures. One unusual aspect is that the atomic coordinations in the hybrid structure are very different from those in the corresponding inorganic component. For instance, in ZnTe(en)_{0.5}, the Te atom is only triply bonded to three Zn, and the Zn atom is bonded to three Te and one N atom, which makes it nontrivial to use any empirical technique (e.g., EPM) for computing the electronic structure. While a density-function theory can handle such structures without much difficulty, the well-known errors due to the local density approximation (LDA) and other limitations hinder our ability to quantitatively account for the electronic and optical properties. Especially, the large exciton binding energy implies the need to involve the whole BZ in order to treat properly the excitonic effect in the optical properties. A full GW calculation is in-principle suitable for such a task, but in practice it is computationally very expensive.

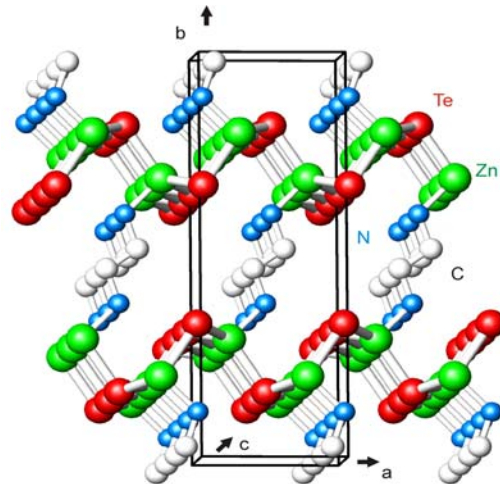


Figure 1. The crystal structure of β -ZnTe(en)_{0.5}. Two-monolayer-thick (110) ZnTe slabs are interconnected by ethylenediamine (en) molecules bounded to Zn atoms. Hydrogen atoms are omitted for clarity.

Additionally, it is important to understand the kinetic effect that determines the phase selectivity in synthesis,⁵ and the dependence of the material stability on the crystal structure and inorganic component.

The type II core-shell semiconductor nanowires are of great interest for applications in solar energy (e. g., solar cells, sensitized solar cells, and photoelectrochemical cells for hydrogen generation via water splitting) and thermoelectricity.^{6, 7} Suitable materials combinations may be, for example, GaN-GaP, ZnO-ZnSe, CdSe-CdTe. Because of the unusual geometry, strain and atomic relaxation, empirical techniques are generally not suitable for these structures. Also because of the type-II energy alignment, the LDA errors are more problematic than in simpler structures (e.g., single component nanowires). Conventional density function theories have been applied to such nanowires, with empirical corrections made for the non-local pseudopotentials to correct the band structure of the bulk binary semiconductors. Figure 2 shows the calculated band edge electron and hole wavefunctions in GaN-GaP and GaP-GaN core-shell nanowires.⁶ However, the calculations are limited to nanowire sizes of a few hundred atoms/period (< 3 nm in the wire diameter), which are significantly smaller than those of nanowires that have been synthesized and studied experimentally. It remains challenging to compute and understand a few important physical properties other than the basic electronic band structure. For instance, finding optimized surface passivation agents (currently pseudo-hydrogen atoms are usually used for eliminating the surface states within the bandgap), energy alignments with respect to other semiconductors with which the nanowires may interact, the excitonic effect, dielectric functions, the stability of the nanowires.

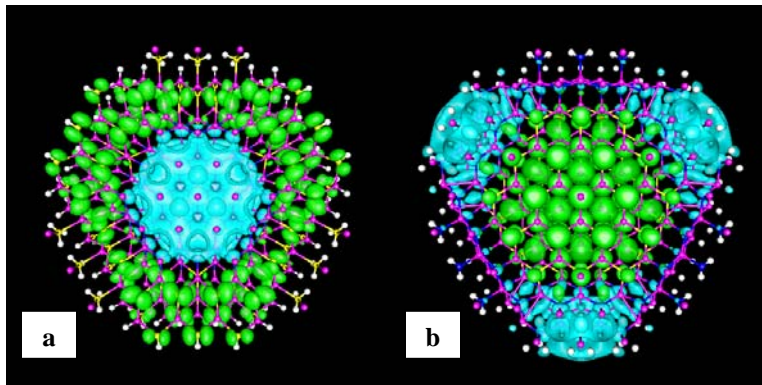


Figure 2. The cross-section views of charge distributions of the CBM electron state (cyan) and VBM hole state (green) in core-shell nanowires. (a) GaN(core)-GaP(shell), (b) GaP(core)-GaN(shell). The color codes are N – blue, P – yellow, Ga – magenta, H – white.

References

- ¹ X. Y. Huang, J. Li, Y. Zhang, et al., *J. Am. Chem. Soc.* 125, 7049 (2003).
- ² Y. Zhang, G. M. Dalpian, B. Fluegel, et al., *Phys. Rev. Lett.* 96, 026405 (2006).
- ³ B. Fluegel, Y. Zhang, A. Mascarenhas, et al., *Phys. Rev. B* 70, 205308 (2004).
- ⁴ Y. Zhang et al., *Phys. Rev. Lett.* (in press).
- ⁵ C. Y. Moon, G. M. Dalpian, Y. Zhang, et al., *Chem. Mat.* 18, 2805 (2006).
- ⁶ Y. Zhang, L.-W. Wang, and A. Mascarenhas, *Nano Lett.* 7, 1264 (2007).
- ⁷ J. Schrier, D. O. Demchenko, L.-W. Wang, et al., *Nano Lett.* (2007).

Novel Thermomechanical Responses of One-dimensional Semiconducting Nanomaterials

Min Zhou

The George W. Woodruff School of Mechanical Engineering and
The School of Materials Science and Engineering
Georgia Institute of Technology, Atlanta, Georgia 30332-0405, USA
Tel: 404-894-3294, Fax: 404-894-0186, Email: min.zhou@gatech.edu

Recently, we showed that polymorphism in semiconducting compounds such as ZnO and CdSe (groups II-VI), GaN and InN (III-V) and SiC (IV-IV) is much more pronounced than previously known. This finding highlights the fact that the crystalline structures of a material reflect a complex interplay of intrinsic factors such as composition, band structure, valence electrons, bonding states and structural symmetry and extrinsic factors such as temperature and loading. A change in any of these factors may trigger a transformation to a different structure. In particular, our recent finding concerns the dependence of the electronic bonding states of these compounds on applied loading. For example, there are three hitherto known polymorphs of ZnO, including wurtzite (WZ), rock salt (RS) and zinc blende (ZB). We discovered two new polymorphs of ZnO as the results of phase transformations from WZ in nanowires under tensile loading. One is a graphitic structure (referred to as HX) in $[01\bar{1}0]$ -orientated nanowires and the other is a body-centered-tetragonal structure (referred to as BCT-4) in $[0001]$ -oriented nanowires. First-principles calculations based on the density functional theory (DFT) and molecular dynamics (MD) simulations have yielded critical conditions for these transformations and have shown that load triaxiality plays an important role in determining phase transformations of ZnO in general. A crystalline structure-load triaxiality map is developed to delineate the relationship between the structures and load condition. The newly identified polymorphic transformations lead to novel pseudoelastic behaviors with recoverable strains up to 16% which were previously unknown for the normally brittle ZnO. The transformations also give rise to a coupling between the thermal and mechanical behaviors of the nanowires and offer mechanisms for developing nanocomponents with tunable responses. In particular, the WZ-to-HX transformation provides for variations in thermal conductivity of up to 100% through the application of a mechanical input.

References:

1. A. J. Kulkarni, K. Sarasamak, S. Limpijumnong and M. Zhou, Characterization of novel pseudoelastic behavior of zinc oxide nanowires, *Philosophical Magazine*, **87**(14), 2117-2134, 2007;
2. A. J. Kulkarni, M. Zhou, K. Sarasamak and S. Limpijumnong, Novel phase transformation in ZnO nanowires under tensile loading, *Physical Review Letters*, **97**, 105502, 2006;
3. A. J. Kulkarni and M. Zhou, Surface-effects-dominated thermal and mechanical responses of zinc oxide nanobelts, *Acta Mechanica Sinica*, **22**(3), 217-224, 2006;
4. A. Kulkarni and M. Zhou, Size-dependent thermal conductivity of Zinc Oxide Nanobelts, *Applied Physics Letters*, **88**, 141921, 2006;
5. A. Kulkarni, M. Zhou and F. J. Ke, Orientation and size dependence of the elastic properties of zinc oxide nanobelts, *Nanotechnology*, **16**, 2749-2756, 2005
6. A. J. Kulkarni and M. Zhou, Tunable thermal response of ZnO nanowires, *Nanotechnology*, accepted for publication and to appear, 2007.

**nanoHUB.org –
Future Cyberinfrastructure serving over 26,000 users today
with online simulation and more**

Gerhard Klimeck

Network for Computational Nanotechnology (NCN), Purdue University, W. Lafayette, IN 47907

The U.S. National Science Foundation envisions future cyberinfrastructures to be built on the four pillars of virtual organizations, high performance computing, visualization and data. nanoHUB.org embodies such a cyberinfrastructure today that serves over 26,000 users worldwide on an annual basis. Over 5,900 of these users have run over 219,000 simulations, including HPC-based runs and visualized data interactively with the over 50 available applications. nanoHUB is used by all top 50 US engineering schools. The nanoHUB provides the resources for modeling, simulating and computing without any software installation to users with access to a web browser. All nanoHUB services are freely open to the public. The nanoHUB represents a community-based, service-oriented, science architecture that leads the way for new cyberinfrastructure-enabled science. We have identified 81 citations in the literature by non-nanoHUB affiliated scientists and engineers.

This presentation will provide a nanoHUB overview and demonstrate how effective, user-friendly cyberinfrastructure can bridge education and research seamlessly for computational experts, experimentalists, educators, and students. Several tools will be demonstrated such as the quantum dot lab, CNTbands, Schred, and nanowire. All these tools have found extensive use in the community in education and research. All but the nanowire code execute in virtually interactive computation times of seconds. The nanowire tool utilizes the Open Science Grid computing resources and delivers results that can be visualized interactively in a few hours. Full fledged versions of NEMO 3-D will be deployed shortly for expert users.

The presentation will conclude with a vision for future expansions into HUBs for other fields. ThenanoHUB and HUBzero team are continually looking for a few bright minds that want to put their expertise into use – we are looking for student or professional software developers in the areas of applications, HPC, performance optimization, visualization, virtualization, and general web development.